

**Figure 3.** S1P<sub>1</sub> expression in *Ccr7*<sup>-/-</sup> T<sub>reg</sub> cells. **A:** Western blotting of S1P<sub>1</sub> in T<sub>reg</sub> cells from WT and *Ccr7*<sup>-/-</sup> mice (*n* = 3/group) was performed. GAPDH expression was used as a housekeeping protein. **B:** Relative expression of S1P<sub>1</sub> to GAPDH was quantified using the protein band intensities in A. Data are presented as means ± SD (*n* = 3). **C:** Phosphorylation of Rac-1 in T<sub>reg</sub> cells of LNs from WT and *Ccr7*<sup>-/-</sup> mice was analyzed under confocal microscopy. Nuclei were stained with DAPI. Images are representative of three mice in each group. Scale bar = 10 μm. **D:** Western blot analysis of Rac-1 and phosphorylated Rac-1 was performed. Results are representative of three independent experiments. **E:** Migration assay of WT and *Ccr7*<sup>-/-</sup> T<sub>reg</sub> cells was performed using anti-CD3 mAb (0.5 mg/mL), S1P (100 nmol/L), CCL19 (50 ng/mL), CCL21 (50 ng/mL), and pretreatment (6 hours) with FTY720 or PTX. Data are presented as means ± SD (*n* = 3) and are representative of three independent experiments. \**P* < 0.05.

with anti-CD3 mAb in the presence of S1P (Figure 5A). In support of these findings, the immunoblot analysis showed much stronger phosphorylation of c-Jun in WT T<sub>reg</sub> cells stimulated with anti-CD3 mAb and S1P than in *Ccr7*<sup>-/-</sup> T<sub>reg</sub> cells (Figure 5B). Furthermore, the transcriptional activity of c-Jun was significantly increased using nuclear extracts from WT T<sub>reg</sub> cells stimulated with anti-CD3 mAb and S1P, compared with extracts from *Ccr7*<sup>-/-</sup> T<sub>reg</sub> cells (Figure 5C). These results show that the CCR7-dependent TCR/CD3-S1P/S1P<sub>1</sub> signaling pathway is critical for T<sub>reg</sub> function through AP-1 activation.

To examine whether the transcriptional activity of c-Jun is controlled by CCR7 ligands (CCL21 and CCL19), we analyzed the activity of WT T<sub>reg</sub> cells stimulated with

anti-CD3mAb in the presence of both S1P and CCL21 or CCL19. The transcriptional activity of c-Jun in anti-CD3mAb-engaged T<sub>reg</sub> cells was enhanced by S1P and CCL21 or CCL19 (Figure 6, A and B). On the other hand, the transcriptional activity of c-Jun of *Ccr7*<sup>-/-</sup> T<sub>reg</sub> cells was enhanced by CCR7 ligands, in addition to CD3 engagement and S1P (Figure 6, A and B). These results suggest that the cooperative action of CCR7 signaling with the TCR/CD3-S1P/S1P<sub>1</sub> signaling pathway plays an important role in the AP-1-mediated function of T<sub>reg</sub> cells.

### Abnormal Nuclear Localization of Foxp3 in *Ccr7*<sup>-/-</sup> T<sub>reg</sub> Cells

As a unique finding regarding the localization of Foxp3 in *Ccr7*<sup>-/-</sup> T<sub>reg</sub> cells, Foxp3 was positioned like a ring in the perinuclear region of unstimulated T<sub>reg</sub> cells in *Ccr7*<sup>-/-</sup> mice, whereas in WT T<sub>reg</sub> cells it was positioned in the center of the nucleus (Figure 5A). In further analysis using confocal microscopy, in *Ccr7*<sup>-/-</sup> mice Foxp3 was detected in the nuclear membrane and perinucleus, or a small amount of Foxp3 protein was detected in the cytoplasm near the nuclear membranes of LN T<sub>reg</sub> cells,

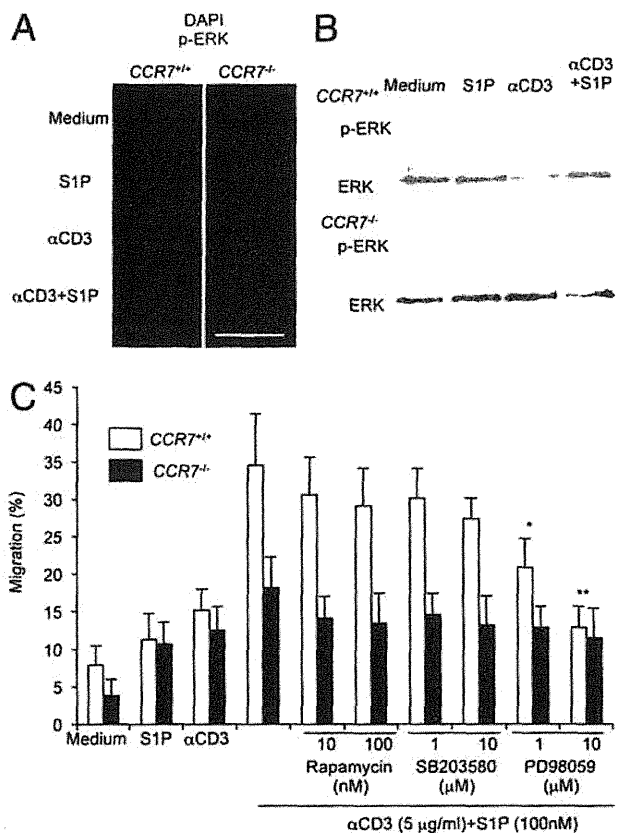


**Figure 4.** Signaling pathway downstream of S1P<sub>1</sub> in *Ccr7*<sup>-/-</sup> T<sub>reg</sub> cells. **A:** Phosphorylation of ERK in Foxp3<sup>+</sup> T<sub>reg</sub> cells of LNs from WT and *Ccr7*<sup>-/-</sup> mice was detected under confocal microscopy. Scale bar = 10 μm. **B:** Phosphorylation of ERK and total ERK in Foxp3<sup>+</sup> T<sub>reg</sub> cells of LNs from WT and *Ccr7*<sup>-/-</sup> mice were detected by Western blotting. **C:** Migration assay of WT and *Ccr7*<sup>-/-</sup> T<sub>reg</sub> cells was performed using anti-CD3 mAb (0.5 mg/mL), S1P (100 nmol/L), CCL19 (50 ng/mL), CCL21 (50 ng/mL), and pretreatment (6 hours) with rapamycin (10 and 100 nmol/L), SB203580 (1 and 10 μmol/L), or PD98059 (1 and 10 μmol/L). Data are presented as means ± SD (*n* = 3) and are representative of three independent experiments. \**P* < 0.05; \*\**P* < 0.005.

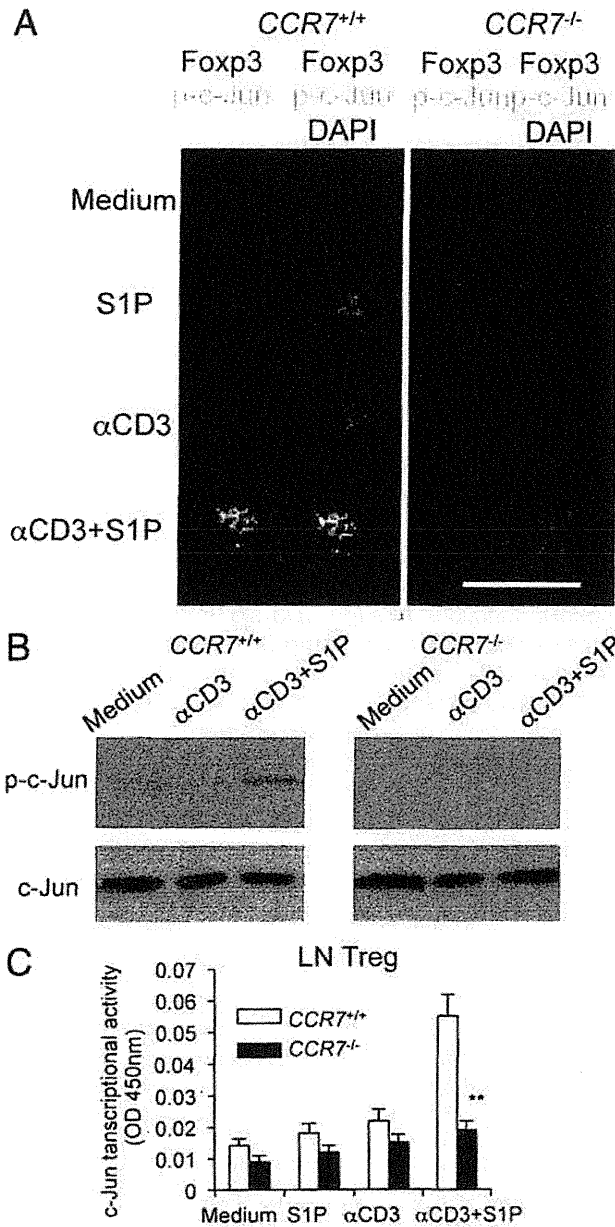


**Figure 5.** MAPK and AP-1 signaling in  $T_{reg}$  cells through S1P<sub>1</sub> and CCR7. **A:** Foxp3 and phospho-c-Jun in LN  $T_{reg}$  cells from WT and  $Ccr7^{-/-}$  mice were analyzed under confocal microscopy. Nuclei were stained with DAPI. Results are representative of three independent experiments. Scale bar = 10  $\mu$ m. **B:** Detection of phospho-c-Jun and total c-Jun in LN  $T_{reg}$  cells from WT and  $Ccr7^{-/-}$  mice was analyzed by Western blot. Results are representative of two independent experiments. **C:** c-Jun transcriptional activity of LN  $T_{reg}$  cells from WT and  $Ccr7^{-/-}$  mice was measured using an AP-1 binding probe. Data are presented as means  $\pm$  SD ( $n = 3$ ) and are representative of two independent experiments. \*\* $P < 0.005$  versus WT.

whereas in WT  $T_{reg}$  cells it was present exclusively in the nucleus (Figure 7, A and B). Even when  $Ccr7^{-/-}$   $T_{reg}$  cells were cultured without stimulus (medium only), Foxp3 was localized in the perinuclear region of the cell (Figure 5A). When  $Ccr7^{-/-}$   $T_{reg}$  cells were stimulated with anti-CD3 mAb or anti-CD3 mAb + S1P, Foxp3 was localized both in the perinucleus and in the center of the nucleus (Figure 5A). These findings suggest that CCR7 regulates the nuclear localization of Foxp3. According to a recent report, Foxp3 significantly suppresses the tran-

scriptional activity and promoter DNA binding of AP-1 by interacting with c-Jun, indicating that Foxp3 is a suppressor of c-Jun-based AP-1 transcriptional activity.<sup>11</sup> The binding of Foxp3 to c-Jun in WT  $T_{reg}$  cells stimulated by anti-CD3 mAb and S1P, was observed by immunoprecipitation with anti-Foxp3 mAb; however, this binding was not present in  $Ccr7^{-/-}$   $T_{reg}$  cells (Figure 7C). In contrast, there were no differences in mRNA expression of Foxp3 between WT and  $Ccr7^{-/-}$   $T_{reg}$  cells (Figure 7D). It may be that Foxp3 is localized in the perinuclear region of the cells because of impaired c-Jun activation in  $Ccr7^{-/-}$   $T_{reg}$  cells.

### Discussion

In the present study, we confirmed two possible molecular mechanisms underlying  $T_{reg}$  cell function mediated by CCR7. In one mechanism, our results suggest that the cooperative action of CCR7 with TCR/CD3 controls the internalization of S1P/S1P<sub>1</sub> with Gi after the phosphorylation of c-Jun as well as MAPK activation in  $T_{reg}$  cells (see Supplemental Figure S3 at <http://ajp.amjpathol.org>). The other mechanism shows that Foxp3 can bind to phosphorylated c-Jun in the nucleus to inhibit the transcriptional activity required for the migratory function or unresponsiveness of Treg cells. In contrast, c-Jun unbound from Foxp3 in the nucleus may act as a transcription factor for the migratory function of peripheral  $T_{reg}$  cells (see Supplemental Figure S3 at <http://ajp.amjpathol.org>). We hypothesize that the migratory function of  $T_{reg}$  cells is controlled by c-Jun activation, which is regulated by the S1P/S1P<sub>1</sub> pathway through the cooperative action between TCR/CD3 and CCR7 signaling and the molecular interaction of Foxp3 with c-Jun. In contrast, in  $Ccr7^{-/-}$   $T_{reg}$  cells, defective internalization of S1P/S1P<sub>1</sub> after ac-

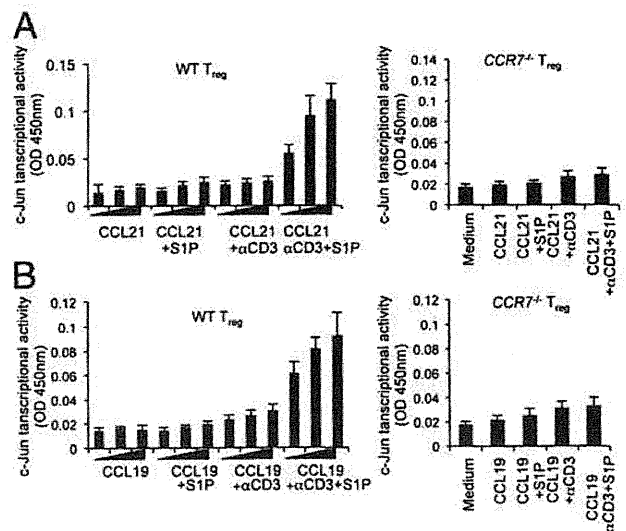


**Figure 6.** Control of c-Jun transcriptional activity in  $T_{reg}$  cells by ligation with CCR7. The c-Jun transcriptional activity of WT and  $Ccr7^{-/-}$   $T_{reg}$  cells stimulated with plate-coated anti-CD3mAb (0.5  $\mu$ g/mL) in the presence of S1P and CCL21 (0, 20, 50 ng/mL) (A) or CCL19 (0, 20, 50 ng/mL) (B) was evaluated. For  $Ccr7^{-/-}$   $T_{reg}$  cells, CCL19 and CCL21 were used (50 ng/mL). Data are presented as means  $\pm$  SD ( $n = 3$ ) and are representative of two independent experiments. OD, optical density.

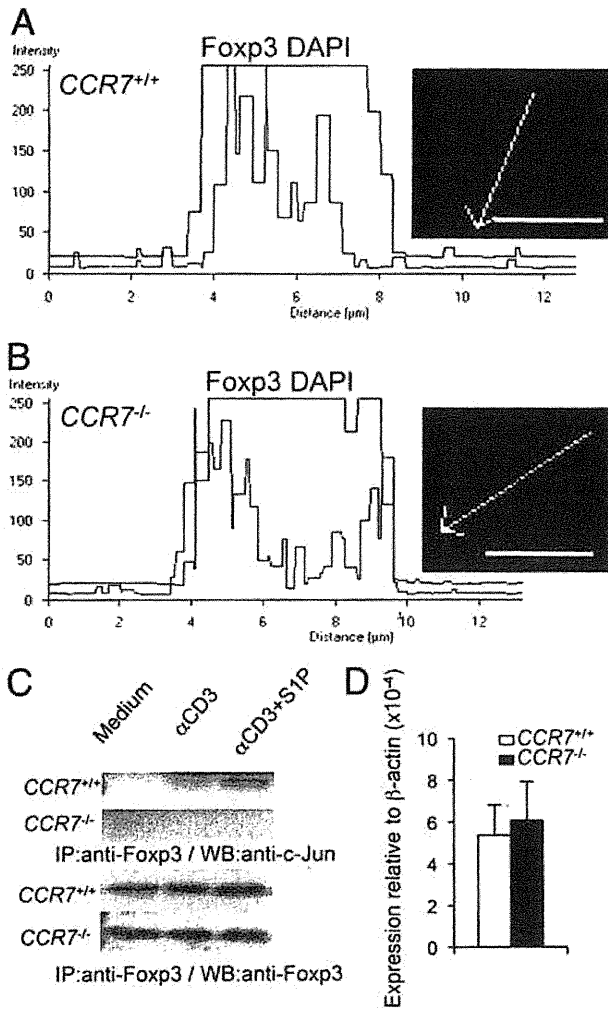


**Figure 7.** Abnormal nuclear localization of Foxp3 and impaired binding of Foxp3 to c-Jun. **A** and **B**: Nuclear localization of Foxp3 was evaluated by confocal microscopy analysis with DAPI staining. Relative fluorescence intensity of Foxp3 and DAPI along the axis of the arrow in the direction pointed by the arrow is shown. Results are representative of two independent experiments. Scale bars = 10 μm. **C**: Impairment of interaction between Foxp3 and c-Jun in Ccr7<sup>-/-</sup> T<sub>reg</sub> cells was detected by immunoprecipitation with anti-Foxp3 mAb and by Western blotting with anti-c-Jun pAb. Results are representative of two independent experiments. **D**: Foxp3 mRNA expression was quantified by real-time PCR. Data are presented as means ± SD (n = 3).

activation of MAPK and c-Jun may result in an impaired migratory response. It was reported that Foxp3 suppresses both the transcriptional activity and promoter DNA-binding of AP-1 by interacting with c-Jun, and this is related to the unresponsiveness of T<sub>reg</sub> cells.<sup>11</sup> Our findings suggest that CCR7/S1P<sub>1</sub> signaling through the interaction of c-Jun and Foxp3 in T<sub>reg</sub> cells controls migratory functions, in addition to the unresponsiveness of T<sub>reg</sub> function. This may explain the defective *in vivo* function of Ccr7<sup>-/-</sup> T<sub>reg</sub> cells.

S1P is one of the natural lysophospholipids that control various functions of immune cells, such as migration, proliferation, and cytokine secretion.<sup>20-23</sup> S1P is secreted by macrophages, mast cells, dendritic cells, and platelets.<sup>24,25</sup> The concentration of S1P is higher in the blood and lymph (range, 0.1 to 3 μmol/L) than in the lymphoid organs and other tissues (range, 3 to 100 nmol/

L).<sup>26,27</sup> The S1P concentration gradient in each organ or tissue can control the chemotactic emigration of thymocytes and egress of lymphocytes from LNs during the differentiation or activation of certain pathological conditions.<sup>28,29</sup> More importantly, the condition of cell surface expression of S1P receptors regulates immune cell functions such as egress from LNs.<sup>30,31</sup> Among the five S1P G protein-coupled receptors (ie, S1P<sub>1</sub>, though S1P<sub>5</sub>), S1P<sub>1</sub> is the major S1P receptor responsible for the direct chemotactic response in T cells.<sup>32-34</sup> S1P<sub>1</sub> expressed on the T-cell surface is internalized when T cells are activated through the binding of S1P-S1P<sub>1</sub>.<sup>17</sup> In the present study, although total expression of S1P<sub>1</sub> in Ccr7<sup>-/-</sup> T<sub>reg</sub> cells was not significantly changed compared with that in WT T<sub>reg</sub> cells, migratory function of WT T<sub>reg</sub> cells in the response to CD3 signaling and S1P was impaired by treatment with a Gi inhibitor. In addition, CCR7 ligand-enhanced migratory response of WT T<sub>reg</sub> cells was also inhibited by treatment with a Gi inhibitor. This finding suggests that CCR7 controls S1P/S1P<sub>1</sub>-mediated T<sub>reg</sub>-specific functions through CD3 signaling. However, the precise mechanism underlying CCR7 and S1P<sub>1</sub> signaling remains to be clarified.

TCR/CD3-dependent stimulation of T cells induces the down-regulation of plasma membrane S1P<sub>1</sub>,<sup>17</sup> and activation of several molecules downstream of S1P<sub>1</sub>, including Rac-1, ERK, and c-Jun, after AP-1 activation plays a critical role in S1P/S1P<sub>1</sub>-mediated T cell functions.<sup>15,35</sup> Our results show that the activation of signaling molecules in MAPK and AP-1 pathways through TCR/CD3 and S1P<sub>1</sub> in Ccr7<sup>-/-</sup> T<sub>reg</sub> cells was abrogated. In addition, CD3/S1P-induced transcriptional activity of c-Jun in normal Treg cells was enhanced by the addition of a CCR7 ligand (CCL21 or CCL19). This result suggests that the possible crosstalk between CCR7 and S1P/S1P<sub>1</sub> signaling plays an important role in TCR/CD3-mediated activation or peripheral T<sub>reg</sub> cell migration. A recent report indicates that S1P<sub>1</sub> delivers an intrinsic negative signal to restrain thymic generation, peripheral maintenance, and suppressive activity of T<sub>reg</sub> cells.<sup>36</sup> Furthermore, it was demonstrated that S1P<sub>1</sub> induces the selective activation of the Akt-mTOR kinase pathway to impede the development and function of T<sub>reg</sub> cells.<sup>15</sup> Although the present study was focused on the migratory function of peripheral T<sub>reg</sub> cells and not the development and function of thymic T<sub>reg</sub> cells, we note that the Akt-mTOR pathway may be associated with the S1P<sub>1</sub>-AP-1 pathway. Because the phosphorylation of ERK in Ccr7<sup>-/-</sup> T<sub>reg</sub> cells was abrogated by stimulation with anti-CD3 mAb and S1P, but ERK activation in WT T<sub>reg</sub> cells was detectable, it is possible that the Akt-mTOR pathway can act at any step in the S1P<sub>1</sub>-AP-1 pathway. Our results show that ERK activation through CCR7/CD3/S1P<sub>1</sub> signaling is more crucial than Akt-mTOR for the migratory functions of T<sub>reg</sub> cells. Further analysis of the molecular interactions between various signaling molecules is warranted.

Foxp3 plays an essential role in suppressing AP-1 DNA-binding activity and consequently inhibiting AP-1 transcription activity, because the expression of Foxp3 significantly blocked AP-1 transcriptional activity and promoter DNA binding.<sup>11</sup> A previous report suggested

that the blocking of AP-1 transcriptional activity by Foxp3 is associated with the unresponsiveness of T<sub>reg</sub> cells because of inhibition of AP-1-mediated activation of T<sub>reg</sub> cells.<sup>11</sup> In addition, transcriptional activation of c-Jun is inhibited in anergic T cells.<sup>37–39</sup> In the present study, signaling after AP-1 activation of *Ccr7*<sup>-/-</sup> T<sub>reg</sub> cells was impaired. As a result, binding of Foxp3 to c-Jun in the nucleus was also undetectable in *Ccr7*<sup>-/-</sup> T<sub>reg</sub> cells. The unresponsiveness of T<sub>reg</sub> cells through the abrogated activation of c-Jun may be related to *in vivo* defects in the function of *Ccr7*<sup>-/-</sup> T<sub>reg</sub> cells, as we have previously reported.<sup>14</sup> Mutations within a putative nuclear localization signal near the C-terminal end of the forkhead domain in the Foxp3 gene abrogate nuclear import of the Foxp3 protein.<sup>40</sup> Although the specific abnormality in the Foxp3 gene of *Ccr7*<sup>-/-</sup> mice is unclear, the impaired signaling of c-Jun by binding Foxp3 in *Ccr7*<sup>-/-</sup> T<sub>reg</sub> cells may influence the localization of the Foxp3 protein. However, it is still unclear whether differentiation in the thymus or maturation in the periphery causes abnormal localization of Foxp3 in the nucleus of *Ccr7*<sup>-/-</sup> T<sub>reg</sub> cells.

In summary, the present data show that CCR7 signaling can control the migratory response of T<sub>reg</sub> cells through a possible crosstalk between Foxp3 and the S1P/S1P<sub>1</sub>-AP-1 pathway. The characterization of this molecular mechanism is important in defining the pathogenesis of autoimmunity based on defects in T<sub>reg</sub> cellular function.

### Acknowledgments

We thank Satoko Katada, Ai Katayama, and Noriko Kino for their technical assistance and Kensuke Takada for the *in vivo* experiments.

### References

- Sakaguchi S: Naturally arising CD4<sup>+</sup> regulatory T cells for immunologic self-tolerance and negative control of immune responses. *Annu Rev Immunol* 2004, 22:531–562
- Sakaguchi S, Yamaguchi T, Nomura T, Ono M: Regulatory T cells and immune tolerance. *Cell* 2008, 133:775–787
- Zheng Y, Rudensky AY: Foxp3 in control of the regulatory T cell lineage. *Nat Immunol* 2007, 8:457–462
- Hori S, Nomura T, Sakaguchi S: Control of regulatory T cell development by the transcription factor Foxp3. *Science* 2003, 299:1057–1061
- Sakaguchi S, Ono M, Setoguchi R, Yagi H, Hori S, Fehervari Z, Shimizu J, Takahashi T, Nomura T: Foxp3<sup>+</sup> CD25<sup>+</sup> CD4<sup>+</sup> natural regulatory T cells in dominant self-tolerance and autoimmune disease. *Immunol Rev* 2006, 212:8–27
- Wan YY, Flavell RA: Regulatory T-cell functions are subverted and converted owing to attenuated Foxp3 expression. *Nature* 2007, 445:766–770
- Zheng Y, Josefowicz SZ, Kas A, Chu TT, Gavin MA, Rudensky AY: Genome-wide analysis of Foxp3 target genes in developing and mature regulatory T cells. *Nature* 2007, 445:936–940
- Li B, Saouaf SJ, Samanta A, Shen Y, Hancock WW, Greene MI: Biochemistry and therapeutic implications of mechanisms involved in FOXP3 activity in immune suppression. *Curr Opin Immunol* 2007, 19:583–588
- Ono M, Yaguchi H, Ohkura N, Kitabayashi I, Nagamura Y, Nomura T, Miyachi Y, Tsukada T, Sakaguchi S: Foxp3 controls regulatory T-cell function by interacting with AML1/Runx1. *Nature* 2007, 446:685–689
- Wu Y, Borde M, Heissmeyer V, Feuerer M, Lapan AD, Stroud JC, Bates DL, Guo L, Han A, Ziegler SF, Mathis D, Benoist C, Chen L, Rao A: FOXP3 controls regulatory T cell function through cooperation with NFAT. *Cell* 2006, 126:375–387
- Lee SM, Gao B, Fang D: FoxP3 maintains Treg unresponsiveness by selectively inhibiting the promoter DNA-binding activity of AP-1. *Blood* 2008, 111:3599–3606
- Kurobe H, Liu C, Ueno T, Saito F, Ohgashi I, Seach N, Arakaki R, Hayashi Y, Kitagawa T, Lipp M, Boyd RL, Takahama Y: CCR7-dependent cortex-to-medulla migration of positively selected thymocytes is essential for establishing central tolerance. *Immunity* 2006, 24:165–177
- Schneider MA, Meingassner JG, Lipp M, Moore HD, Rot A: CCR7 is required for the *in vivo* function of CD4<sup>+</sup> CD25<sup>+</sup> regulatory T cells. *J Exp Med* 2007, 204:735–745
- Ishimaru N, Nitta T, Arakaki R, Yamada A, Lipp M, Takahama Y, Hayashi Y: In situ patrolling of regulatory T cells is essential for protecting autoimmune exocrinopathy. *PLoS One* 2010, 5:e8588
- Liu G, Burns S, Huang G, Boyd K, Proia RL, Flavell RA, Chi H: The receptor S1P1 overrides regulatory T cell-mediated immune suppression through Akt-mTOR. *Nat Immunol* 2009, 10:769–777
- Liao JJ, Huang MC, Graler M, Huang Y, Qiu H, Goetzl EJ: Distinctive T cell-suppressive signals from nuclearized type 1 sphingosine 1-phosphate G protein-coupled receptors. *J Biol Chem* 2007, 282:1964–1972
- Rivera J, Proia RL, Olivera A: The alliance of sphingosine-1-phosphate and its receptors in immunity. *Nat Rev Immunol* 2008, 8:753–763
- Means CK, Miyamoto S, Chun J, Brown JH: S1P1 receptor localization confers selectivity for Gi-mediated cAMP and contractile responses. *J Biol Chem* 2008, 283:11954–11963
- Matsuyuki H, Maeda Y, Yano K, Sugahara K, Chiba K, Kohno T, Igarashi Y: Involvement of sphingosine 1-phosphate (S1P) receptor type 1 and type 4 in migratory response of mouse T cells toward S1P. *Cell Mol Immunol* 2006, 3:429–437
- Goetzl EJ, Rosen H: Regulation of immunity by lysosphingolipids and their G protein-coupled receptors. *J Clin Invest* 2004, 114:1531–1537
- Goetzl EJ, Wang W, McGiffert C, Huang MC, Graler MH: Sphingosine 1-phosphate and its G protein-coupled receptors constitute a multifunctional immunoregulatory system. *J Biol Chem* 2004, 279:1104–1114
- Graeler M, Goetzl EJ: Activation-regulated expression and chemotactic function of sphingosine 1-phosphate receptors in mouse splenic T cells. *FASEB J* 2002, 16:1874–1878
- Graeler M, Shankar G, Goetzl EJ: Cutting edge: suppression of T cell chemotaxis by sphingosine 1-phosphate. *J Immunol* 2002, 169:4084–4087
- Olivera A, Rivera J: Sphingolipids and the balancing of immune cell function: lessons from the mast cell. *J Immunol* 2005, 174:1153–1158
- Pappu R, Schwab SR, Cornelissen I, Pereira JP, Regard JB, Xu Y, Camerer E, Zheng YW, Huang Y, Cyster JG, Coughlin SR: Promotion of lymphocyte egress into blood and lymph by distinct sources of sphingosine-1-phosphate. *Science* 2007, 316:295–298
- Lee MJ, Van Brocklyn JR, Thangada S, Liu CH, Hand AR, Menzeleev R, Spiegel S, Hla T: Sphingosine-1-phosphate as a ligand for the G protein-coupled receptor EDG-1. *Science* 1998, 279:1552–1555
- Schwab SR, Pereira JP, Matloubian M, Xu Y, Huang Y, Cyster JG: Lymphocyte sequestration through S1P lyase inhibition and disruption of S1P gradients. *Science* 2005, 309:1735–1739
- Chiba K, Matsuyuki H, Maeda Y, Sugahara K: Role of sphingosine 1-phosphate receptor type 1 in lymphocyte egress from secondary lymphoid tissues and thymus. *Cell Mol Immunol* 2006, 3:11–19
- Rosen H, Goetzl EJ: Sphingosine 1-phosphate and its receptors: an autocrine and paracrine network. *Nat Rev Immunol* 2005, 5:560–570
- Schwab SR, Cyster JG: Finding a way out: lymphocyte egress from lymphoid organs. *Nat Immunol* 2007, 8:1295–1301
- von Wenckstern H, Zimmermann K, Kleuser B: The role of the lysosphingolipid sphingosine 1-phosphate in immune cell biology. *Arch Immunol Ther Exp (Warsz)* 2006, 54:239–251
- Graler MH, Huang MC, Watson S, Goetzl EJ: Immunological effects of transgenic constitutive expression of the type 1 sphingosine 1-phosphate receptor by mouse lymphocytes. *J Immunol* 2005, 174:1997–2003

33. Matloubian M, Lo CG, Cinamon G, Lesneski MJ, Xu Y, Brinkmann V, Allende ML, Proia RL, Cyster JG: Lymphocyte egress from thymus and peripheral lymphoid organs is dependent on S1P receptor 1. *Nature* 2004, 427:355-360
34. Wang W, Huang MC, Goetzl EJ: Type 1 sphingosine 1-phosphate G protein-coupled receptor (S1P1) mediation of enhanced IL-4 generation by CD4 T cells from S1P1 transgenic mice. *J Immunol* 2007, 178:4885-4890
35. Windh RT, Lee MJ, Hla T, An S, Barr AJ, Manning DR: Differential coupling of the sphingosine 1-phosphate receptors Edg-1, Edg-3, and H218/Edg-5 to the G(i), G(q), and G(12) families of heterotrimeric G proteins. *J Biol Chem* 1999, 274:27351-27358
36. Kim CH: Reining in FoxP3(+) regulatory T cells by the sphingosine 1-phosphate-S1P1 axis. *Immunol Cell Biol* 2009, 87:502-504
37. Kitagawa-Sakakida S, Schwartz RH: Multifactor cis-dominant negative regulation of IL-2 gene expression in anergized T cells. *J Immunol* 1996, 157:2328-2339
38. Powell JD, Lerner CG, Ewoldt GR, Schwartz RH: The -180 site of the IL-2 promoter is the target of CREB/CREM binding in T cell anergy. *J Immunol* 1999, 163:6631-6639
39. Sundstedt A, Sigvardsson M, Leanderson T, Hedlund G, Kalland T, Dohlsten M: In vivo anergized CD4+ T cells express perturbed AP-1 and NF-kappa B transcription factors. *Proc Natl Acad Sci USA* 1996, 93:979-984
40. Lopes JE, Torgerson TR, Schubert LA, Anover SD, Ocheltree EL, Ochs HD, Ziegler SF: Analysis of FOXP3 reveals multiple domains required for its function as a transcriptional repressor. *J Immunol* 2006, 177:3133-3142

# A Novel DC Therapy with Manipulation of MKK6 Gene on Nickel Allergy in Mice

Megumi Watanabe<sup>1,2</sup>, Naozumi Ishimaru<sup>1\*</sup>, Meinar Nur Ashrin<sup>1,2</sup>, Rieko Arakaki<sup>1</sup>, Akiko Yamada<sup>1</sup>, Tetsuo Ichikawa<sup>2</sup>, Yoshio Hayashi<sup>1</sup>

<sup>1</sup> Department of Oral Molecular Pathology, Institute of Health Biosciences, The University of Tokushima Graduate School, Tokushima, Japan, <sup>2</sup> Department of Oral Maxillofacial Prosthodontics, Institute of Health Biosciences, The University of Tokushima Graduate School, Tokushima, Japan

## Abstract

**Background:** Although the activation of dermal dendritic cells (DCs) or Langerhans cells (LCs) via p38 mitogen-activated protein kinase (MAPK) plays a crucial role in the pathogenesis of metal allergy, the *in vivo* molecular mechanisms have not been identified and a possible therapeutic strategy using the control of dermal DCs or LCs has not been established. In this study, we focused on dermal DCs to define the *in vivo* mechanisms of metal allergy pathogenesis in a mouse nickel (Ni) allergy model. The effects of DC therapy on Ni allergic responses were also investigated.

**Methods and Finding:** The activation of dermal DCs via p38 MAPK triggered a T cell-mediated allergic immune response in this model. In the MAPK signaling cascade in DCs, Ni potently phosphorylated MAP kinase kinase 6 (MKK6) following increased DC activation. Ni-stimulated DCs could prime T cell activation to induce Ni allergy. Interestingly, when MKK6 gene-transfected DCs were transferred into the model mice, a more pronounced allergic reaction was observed. In addition, injection of short interfering (si) RNA targeting the MKK6 gene protected against a hypersensitivity reaction after Ni immunization. The cooperative action between T cell activation and MKK6-mediated DC activation by Ni played an important role in the development of Ni allergy.

**Conclusions:** DC activation by Ni played an important role in the development of Ni allergy. Manipulating the MKK6 gene in DCs may be a good therapeutic strategy for dermal Ni allergy.

**Citation:** Watanabe M, Ishimaru N, Ashrin MN, Arakaki R, Yamada A, et al. (2011) A Novel DC Therapy with Manipulation of MKK6 Gene on Nickel Allergy in Mice. PLoS ONE 6(4): e19017. doi:10.1371/journal.pone.0019017

**Editor:** Jacques Zimmer, Centre de Recherche Public de la Santé (CRP-Santé), Luxembourg

**Received:** January 7, 2011; **Accepted:** March 14, 2011; **Published:** April 22, 2011

**Copyright:** © 2011 Watanabe et al. This is an open-access article distributed under the terms of the Creative Commons Attribution License, which permits unrestricted use, distribution, and reproduction in any medium, provided the original author and source are credited.

**Funding:** This study was supported in part by a Grant-in-Aid for Scientific Research (Nos. 17109016, 21390518, and 21791901) from the Ministry of Education, Culture, Sports, Science and Technology of Japan, and research grants from Japan Chemical Industry Association (No. LRI 2005CS02). No additional external funding received for this study. The funders had no role in study design, data collection and analysis, decision to publish, or preparation of the manuscript.

**Competing Interests:** The authors have declared that no competing interests exist.

\* E-mail: ishmaru@dent.tokushima-u.ac.jp

## Introduction

Metal allergy is an inflammatory disease categorized as a delayed-type hypersensitivity (DTH) reaction, similar to contact dermatitis and eczema [1,2]. This skin disease is induced by a complex process involving immune responses of numerous cell types, and cooperation among these cells is crucial for symptom development [3,4].

Among various metals, nickel (Ni), when used in costume jewelry or dental alloys, is the most frequent cause of contact allergy [5–7]. Ni-specific T cell responses are crucial for the development of allergies in human and mouse models [8–10]. However, it is unclear how T cells recognize Ni presented to them by antigen-presenting cells (APCs). In the skin, Langerhans cells (LCs) or dermal dendritic cells (DCs) play fundamental roles as APCs for uptake, processing, and presentation of antigens [11,12]. Although there is no evidence that DCs or LCs can directly clear Ni, these APCs may contribute to a Ni allergic response via other molecular mechanisms.

Ni ions (Ni<sup>2+</sup>) are known to be released from various alloys into the skin and exert proinflammatory and irritant properties as potent allergens or haptens [13,14]. Ni penetrates the skin where it

may associate with epithelial cells or become attached to MHC molecules on LCs or DCs. APCs are activated by certain cytokines such as IL-1 $\beta$  and TNF- $\alpha$  produced by keratinocytes. The cytokines regulate the expression of E-cadherin and chemokines like matrix metalloproteinase (MMP)-9, secondary lymphoid tissue chemokine (SLC), and MIP-3 $\beta$  produced by the APCs [15–18]. Subsequently, APCs migrate to draining lymph nodes where they present haptens to naïve T cells. Re-exposure to the same hapten leads to a hypersensitivity reaction in an effector phase.

Recent *in vitro* experiments have reported that contact sensitizers like Ni activate epidermal DCs or LCs as shown by the upregulation of CD80, CD83, CD86, and MHC class II [19]. Moreover, *in vitro* experiments using human DCs showed that Ni-induced phosphorylation of p38 mitogen-activated protein kinase (MAPK) was critical for the maturation of immature DCs [20–22]. In addition, the conditional induction of a dominant active form of MAP kinase kinase 6 (MKK6) efficiently induced the activation of human LCs [23]. However, it remains uncertain whether the *in vivo* activation of DCs in the skin is induced by Ni via the MAPK signaling pathway. Furthermore, it is unclear whether the signaling pathway of DCs stimulated by Ni is different from that of the other stimuli with regard to signal strength or the pathway itself.

The aim of this study was to determine the signaling pathway for APC activation in dermal immune responses related to the pathogenesis of Ni allergy in a mouse model. In addition, a therapeutic strategy based on the *in vivo* molecular mechanisms of Ni allergy was applied to this model.

## Results

### Induction of Hypersensitive Reactions to NiCl<sub>2</sub>

To induce hypersensitive reactions to Ni, Ni is typically applied to the skin surface as a secondary challenge after sensitization. In the first series of experiments, we evaluated results of the mouse ear swelling test, as described previously [24]. Using this protocol (Figure 1A), we found flare reactions and slight increases in ear swelling in response to NiCl<sub>2</sub> (Figure 1B).

In order to elucidate the symptoms associated with hypersensitive reactions to NiCl<sub>2</sub>, we administered intradermal injections into the ear pinnae of mice as previously described [25]. Although attempts to induce Ni allergy in mice have often failed, a DTH reaction to Ni has been achieved after injecting NiCl<sub>2</sub> in combination with an adjuvant or irritant [25]. Thus, we attempted to induce DTH by injecting NiCl<sub>2</sub> in combination with either incomplete Freund's adjuvant (IFA) or complete Freund's adjuvant (CFA) (Figure 1C). A DTH reaction to NiCl<sub>2</sub> was induced in C57BL/6 (B6) female mice using the method shown in Figure 1C.

Briefly, NiCl<sub>2</sub> with IFA was intraperitoneally injected into B6 mice for initial immunization. Two weeks later, NiCl<sub>2</sub> together with CFA was intradermally injected into the ear skin for a recall immune response. DTH reactions were determined by measuring the changes in ear thickness 48 hours after the challenge.

Although increased ear thickness of Ni-treated mice after injection of Ni with IFA has been previously reported [25], in this study, ear swelling was only around 0.2 to 0.3 mm (Figure 1D). In contrast, the ear thickness of Ni+CFA-treated mice after Ni with IFA was significantly higher compared with that of CFA-treated and other mice (Figure 1D). Redness and swelling of the ear skin was observed in Ni+CFA-treated mice after Ni with IFA (Figure 1E). Histological examination of the ear epidermis of Ni+CFA-treated mice after Ni with IFA showed edema, congestion, and extensive infiltration of inflammatory cells, including mononuclear cells, monocytes, neutrophils, and macrophages, in the connective and muscular tissues; however, there was no inflammation in control ears (Figure 1F, Figure S1A). In addition, toluidine blue-positive cells, including degranulated mast cells, found in the lesions of Ni allergy mice were significantly increased compared with those in control mice (Figure S1B). This Ni allergy model with severe inflammation was used to analyze the cellular mechanisms and to develop a therapeutic strategy.

### Cellular Mechanisms of Ni Allergy

To characterize Ni allergy, immune responses to another antigen or metal were compared with Ni immune responses in the present allergy model. Briefly, NiCl<sub>2</sub> or the control metal/antigen (PBS, ovalbumin [OVA], or TiO<sub>2</sub> [Ti]), along with IFA, was intraperitoneally injected into B6 mice. Titanium has been known as one of biocompatible metals, and so it is believed that the allergic sensitivity induced by nickel is rarely occurred by titanium [26]. Therefore, titanium was used as a control metal in this study. Two weeks later, NiCl<sub>2</sub> or the abovementioned control metal/antigen, along with CFA, was intradermally injected into the mice. At 24 and 48 hours after immunization, DTH reactions were assessed by measuring ear thicknesses. In contrast to the swelling seen in OVA- or Ti-treated mice, the ear thicknesses of Ni-treated

mice were significantly increased at both 24 and 48 hours after the second challenge (Figure 2A).

Flow cytometry was performed to identify the phenotypes of infiltrating lymphocytes in the allergic lesions. Large numbers of CD3<sup>+</sup> T cells and CD19<sup>+</sup> B cells were detected in the tissue samples obtained from NiCl<sub>2</sub>-injected mice (Figure 2B). In addition, immunohistochemical analysis indicated that a much higher proportion of CD3<sup>+</sup> T cells were observed in the skin tissues of NiCl<sub>2</sub>-injected mice, compared with CD19<sup>+</sup> B cells (Figure 2C). The infiltrating T cells were largely CD4<sup>+</sup> T cells, with small numbers of CD8<sup>+</sup> T cells and NK1.1<sup>+</sup> natural killer (NK) cells (Figure S2A). Moreover, the proportion of NKT cells reactive to anti- $\alpha$ -GalCer-CD1d complex in the ear tissues of NiCl<sub>2</sub>-injected mice was significantly increased compared with that of control mice (Figure S2B). The number of MHC class II<sup>+</sup>CD11c<sup>+</sup> dermal DCs was significantly higher in NiCl<sub>2</sub>-injected mice than in control mice (Figure 2D). In addition, the absolute numbers of dermal DCs in NiCl<sub>2</sub>-injected mice were significantly increased compared with those in control mice (Figure 2E). In contrast, the number of DCs in the cervical lymph nodes of Ni-injected mice was not increased (Figure S2C). These results suggest that T cells and dermal DCs in the skin lesions play important roles in the development of the hypersensitivity reaction induced by NiCl<sub>2</sub>.

### Activation of DCs by NiCl<sub>2</sub> via MAPK

Numerous signaling molecules control the maintenance of DCs in peripheral tissues [27]. Among these, MAPK is known to be a key signal transducer for the activation of DCs in various immune responses [28,29]. Regarding DCs in allergic reactions in humans, p38/MKK6 in the MAPK pathway plays a significant role in the activation of DCs during the development of skin allergy [23]. Thus, we focused on p38/MKK6 of DCs in mice. To define *in vivo* p38/MKK6 activation of dermal DCs in our Ni allergy model, Western blot analysis of MKK6 was performed using skin tissue samples. MKK6 phosphorylation was significantly increased in the skin tissues of NiCl<sub>2</sub>-injected mice (Figure 3A), but absent in the skin tissues of PBS-, OVA-, and TiO<sub>2</sub>-injected mice (Figure 3A). Further, phospho-MKK6 was detected in MHC class II<sup>+</sup> DCs in the skin tissues of NiCl<sub>2</sub>-injected mice (Figure 3B). These results showed that dermal DC activation via MKK6 was important for the pathogenesis of Ni allergy in the skin.

On the other hand, when phosphorylation of MKK6 and p38 in bone marrow-derived cells (BMDCs) stimulated with NiCl<sub>2</sub> was examined by Western blot analysis, the phosphorylated levels of MKK6 and p38 in NiCl<sub>2</sub>-stimulated BMDCs were elevated similar to those in LPS-stimulated BMDCs (Figure S3A). When stimulated with TiO<sub>2</sub>, however, no phosphorylation of MKK6 and p38 was detected (Figure S3A). We used real-time PCR to examine the MKK6 mRNA expression in BMDCs stimulated with NiCl<sub>2</sub>. The mRNA expression level of MKK6 in BMDCs stimulated with NiCl<sub>2</sub> was increased in a time-dependent manner; it was much higher than that in LPS-stimulated BMDCs during the first 24 hours (Figure S3B), but decreased after 36 hours (Figure S3B). These results showed that Ni could directly trigger the activation of DCs via p38/MKK6 to induce an allergic immune reaction.

### Enhanced Allergy after Transfer of T Cells Primed by NiCl<sub>2</sub>-stimulated DCs

As shown in Figure 2, a large number of T cells had infiltrated into the lesions of inflamed skin tissues. In addition, when purified T cells from the lymph nodes of the Ni allergy model were stimulated with anti-CD3 mAb, production of Th1-type cytokines, including IL-2 and IFN- $\gamma$ , was significantly increased compared

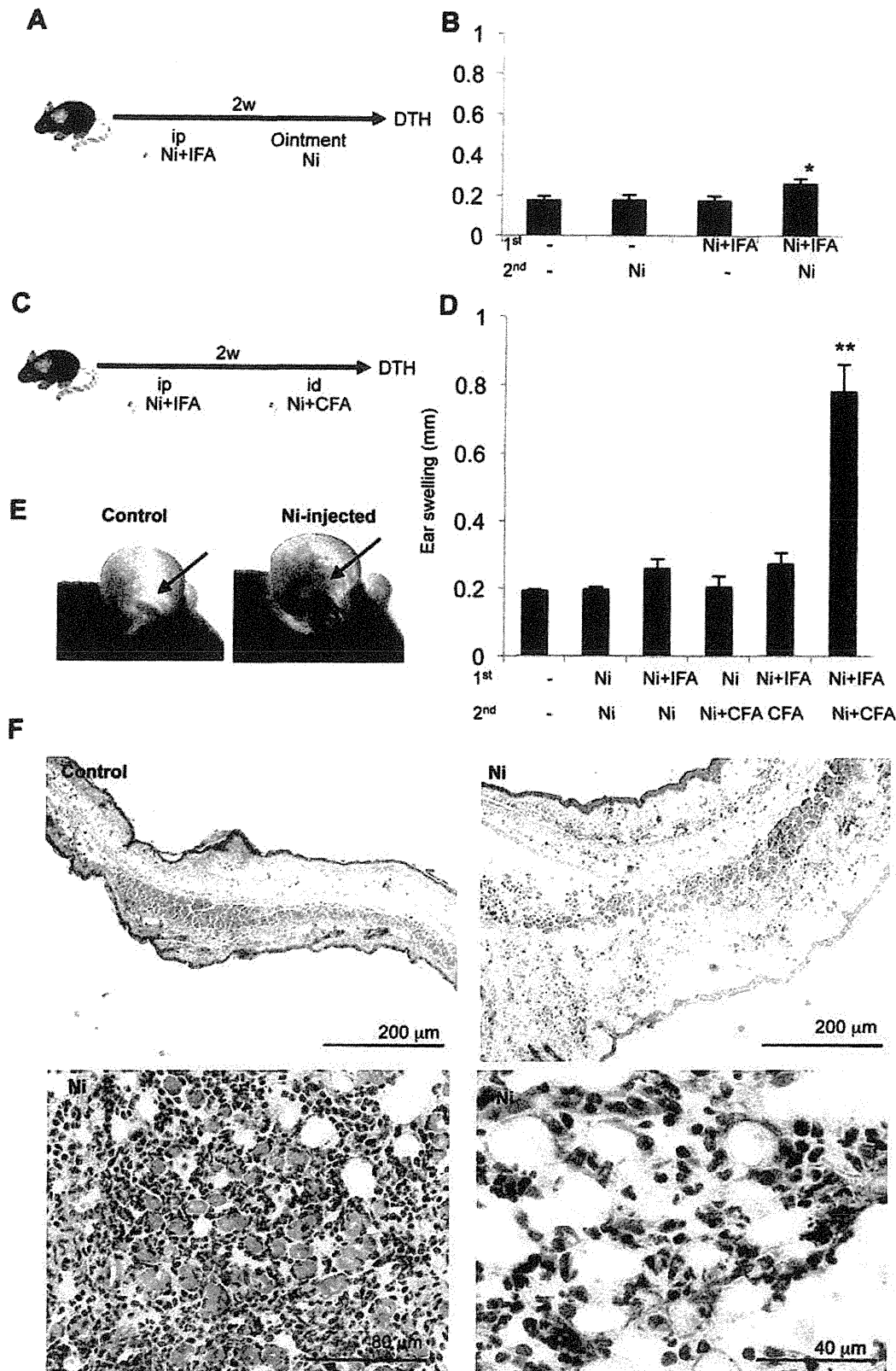


**Figure 1. Induction of Ni allergy.** (A) Protocol for inducing the Ni allergy model. First, an intraperitoneal injection of  $\text{NiCl}_2$  with or without IFA was administered. After 2 weeks, an ointment (o) of  $\text{NiCl}_2$  with Vaseline was applied to the ear pinnae as a secondary challenge. (B) DTH was assessed by measuring the ear thickness at 48 hours after the last challenge. Results are means  $\pm$  SD for 4 mice in each group. (C) Protocol for inducing a Ni allergy model. First, an intraperitoneal injection of  $\text{NiCl}_2$  with or without IFA was administered. Then, after 2 weeks, an intradermal injection of  $\text{NiCl}_2$  with or without CFA was administered to the ear pinnae to induce a secondary reaction. (D) DTH was assessed by measuring the ear thickness at 48 hours after the last challenge. Results are means  $\pm$  SD for 4 to 6 mice in each group. \*\* $P < 0.005$ . (E) Representative photos of the ears from control and  $\text{NiCl}_2$ -injected mice. (F) Histological images of inflammatory lesions in the skin are representative of 5 mice in each group. doi:10.1371/journal.pone.0019017.g001



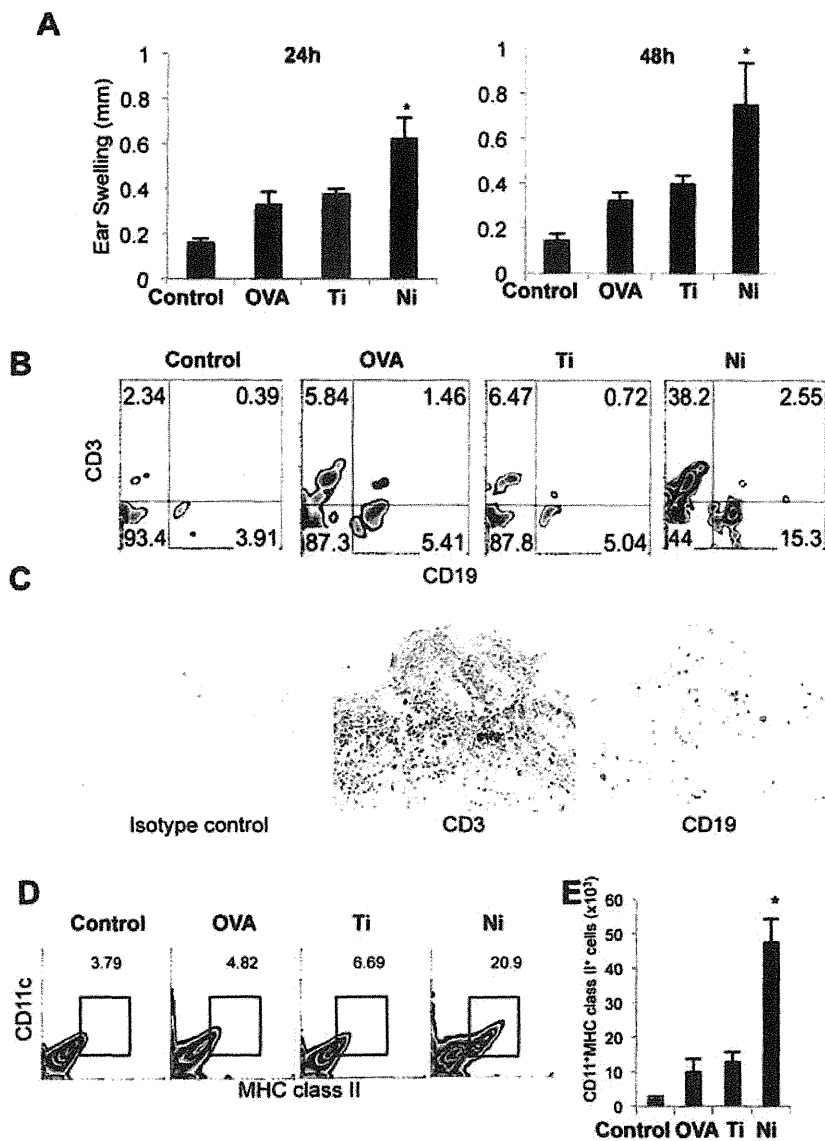


**Figure 2. Characteristics of the Ni allergy model.** (A) DTH was evaluated by measuring the ear thickness of the treated mice. Results are means  $\pm$  SD for 5 mice in each group. \* $P < 0.05$ . (B) T and B cell populations of purified lymphocytes from skin tissues were analyzed by flow cytometry. Representative results of 5 mice in each group are shown. (C) Immunohistochemical analysis of T and B cells was performed on frozen sections of inflamed ear tissues obtained from Ni allergy mice. Representative photos of 2 independent experiments are shown. (D) Dermal DCs were detected by flow cytometry. These results represent 2 independent experiments with 3 mice in each group. (E) The absolute numbers of dermal DCs were determined. \* $P < 0.05$ . doi:10.1371/journal.pone.0019017.g002

with that in controls (Figure S4). On the other hand, the secretion of Th2-type cytokines such as IL-4 and IL-10 from anti-CD3 mAb-stimulated T cells of Ni allergy model was similar to that of the other control mice (Figure S4). These findings suggest that T cells play a key role as effector cells in the pathogenesis of Ni allergy. However, it was still unclear how Ni-stimulated DCs were related to T cell responses in allergic reactions.

Thus, T cells purified from the spleens of normal B6 mice were co-cultured with Ni-stimulated BMDCs *in vitro* for 24 hours. Then, the resulting primed T cells were transferred intraperitoneally into normal B6 mice, and 2 weeks later, NiCl<sub>2</sub> with CFA was injected intradermally to induce DTH (Figure 4A). The skin thickness of the model mice with transferred Ni-BMDCs-stimulated T cells was significantly increased compared with that of mice with transferred nonstimulated T cells (Figure 4B). Pathological examination of the

skin lesions in the mice with transferred Ni-BMDCs-stimulated T cells showed more severe inflammation, including lymphocyte infiltration, edema, and congestion, compared with those in the mice with transferred nonstimulated T cells (Figure 4C). These results suggested that the T cells primed by Ni-stimulated DCs were important for the onset of Ni allergy.

#### Effects of Overexpression of MKK6 in DCs on Ni Allergy

To examine whether DCs activated by the engagement of p38/MKK6 signaling influenced the development of skin allergy, BMDCs were transfected with the MKK6 gene (MKK6-DC) and stimulated with NiCl<sub>2</sub> for 48 hours. Then, MKK6-DCs were subcutaneously transferred into normal B6 mice, and 2 weeks later, NiCl<sub>2</sub> was intradermally injected to induce Ni allergy (Figure 5A). The skin redness in MKK6-DC-transferred mice was

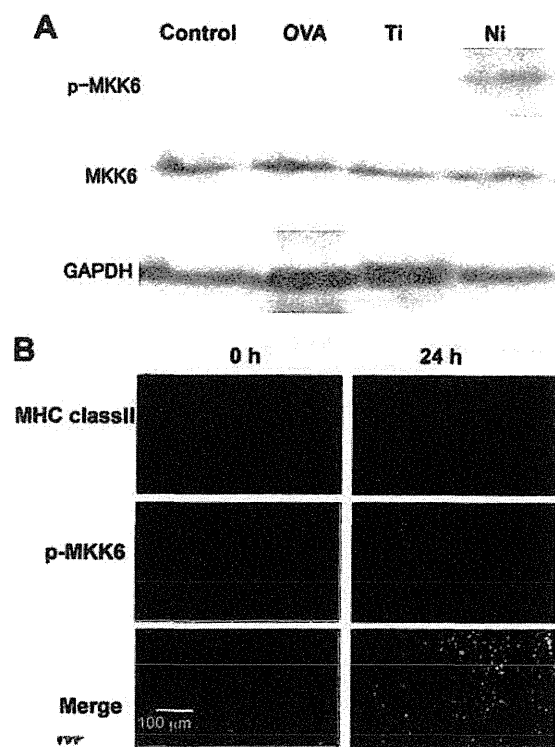


**Figure 3. DC activation by Ni via MKK6.** (A) Phosphorylation of MKK6 in the inflamed tissues of the Ni allergy model was analyzed by Western blot analysis. GAPDH was used as the internal control. (B) Phosphorylation of MKK6 (Red) of MHC class II<sup>+</sup> (Green) dermal DCs from Ni allergy mice was detected by confocal microscopy. These results represent 2 independent experiments with 3 to 5 mice in each group.

doi:10.1371/journal.pone.0019017.g003

enhanced compared with that in Mock-DC-transferred mice (Figure 5B). In addition, pathological examination revealed remarkable infiltration of immune cells along with congestion and edema in the skin lesions of MKK6-DC-transferred mice (Figure 5C). Significantly enhanced ear swelling was detected within 48 hours of injecting NiCl<sub>2</sub> into MKK6-DC-transferred mice compared with Mock-DC-transferred mice (Figure 5D). In addition, we investigated production of cytokines by Ni-stimulated DCs that are required for T cell priming, including IL-12, IFN- $\gamma$ , and IL-10. The amounts of IL-12, IFN- $\gamma$ , and IL-10 produced by BMDCs after stimulation with NiCl<sub>2</sub> were equal to those after stimulation with LPS (Figure S5), and the cytokine production by NiCl<sub>2</sub>-stimulated BMDCs were significantly higher compared with that by TiO<sub>2</sub>-stimulated BMDCs (Figure S5). These results suggested that Ni-mediated DC activation played a central role in T cell priming for the onset and development of Ni allergy.

#### Effective Therapy for Ni Allergy using MKK6 siRNA

We next tested a therapeutic strategy for Ni allergy using short interfering (si) RNA targeting the MKK6 gene. Before inducing a DTH reaction, MKK6 siRNA with atelocollagen as an *in vivo* gene delivery system was subcutaneously injected into the ear skin of the model mice. Ear thickness was measured at 48 hours after injecting NiCl<sub>2</sub> or saline control (Figure 6A). We confirmed that the MKK6 mRNA level in siRNA-treated DCs was significantly reduced (<1/6) compared with that in control siRNA-treated DCs (data not shown).

Ear thickness of MKK6 siRNA-treated allergy model mice was significantly reduced compared with those of control siRNA-treated mice (Figure 6B). In addition, pathological examination showed no detectable inflammatory lesions in MKK6 siRNA-treated mice, while severe inflammation with extensive lymphocytic infiltration, edema, and congestion was observed in the lesions of the mice injected with control siRNA (Figure 6C). Further, although phosphorylation of MKK6 of MHC class II<sup>+</sup> dermal DCs in the skin sheets from MKK6 siRNA-treated mice was nearly undetectable, there was phosphorylation in the sheets from control siRNA-treated mice (Figure 6D). This showed that an effective therapy using siRNA targeting the MKK6 gene could be used for treating Ni allergy.

#### Discussion

DCs in the epidermis and dermis participate in the recognition of pathogens. The two major populations of DCs present in normal skin are epidermal LCs and dermal DCs. These DCs function as APCs and play key roles in sensing pathogens and initiating allergic responses. Immature DCs, such as epidermal LCs, reside in the peripheral tissues. When these DCs are activated by antigens and mature, they migrate from peripheral sites to lymphoid organs where they stimulate T cells to induce an immune response [11,30]. The cutaneous immune system depends on multiple cell-cell contacts for antigen recognition and presentation, as well as inflammation. LCs facilitate the development of contact hypersensitivity responses by efficiently presenting haptens to T cells [31]. However, it has been suggested that dermal DCs can support LC functions [31].

From our results and those of other studies, allergy symptoms, such as swelling and flare reactions, were minimal and transient after applying a Ni-based ointment to the skin surface. Artik et al. demonstrated contact hypersensitivity in model mice after intradermally injecting Ni into the ear pinnae [25]. Our method using intradermal injections of Ni with CFA in a new DTH model was based on their report. Clinical skin tests (such as puncture tests and intradermal injection tests) along with patch tests have been used for the diagnosis of metal allergy. Therefore, we injected NiCl<sub>2</sub> with CFA intradermally into mice in order to obtain clear hypersensitivity responses.

p38 MAPK is an evolutionarily highly conserved stress response pathway in various cells [32]. p38 MAPK is activated by an upstream kinase (MKK6 or MKK3) and then translocated into the nucleus where target molecules are phosphorylated by p38 MAPK [33,34]. A previous report showed that activation of human LCs was triggered by MKK6 [23]. In addition, several reports using *in vitro* experiments showed that p38 MAPK phosphorylation played an important role in the activation of DCs by Ni [34–36]. Our experiments using a Ni allergy model strongly suggest that MKK6 phosphorylation in dermal DCs is the first important trigger for the onset of an allergic response to Ni.

Ni is the most frequent cause of metal allergy. It is possible that Ni in the skin may interact with proteins, after which dermal DCs capture the Ni-antigen complex. At this stage, Ni might be a potent factor for triggering activation of DCs via MKK6. In our model, the specific activation of MKK6 in DCs was observed only when the cells were stimulated with Ni but not another metal or antigen such as Ti or OVA. However, because the phosphorylation of MKK6 in DCs was detectable after stimulation with LPS *in vitro*, the signaling pathway induced by Ni could be modulated by other stimuli. In addition, we could not identify the mechanism by which Ni modulated MKK6 expression.

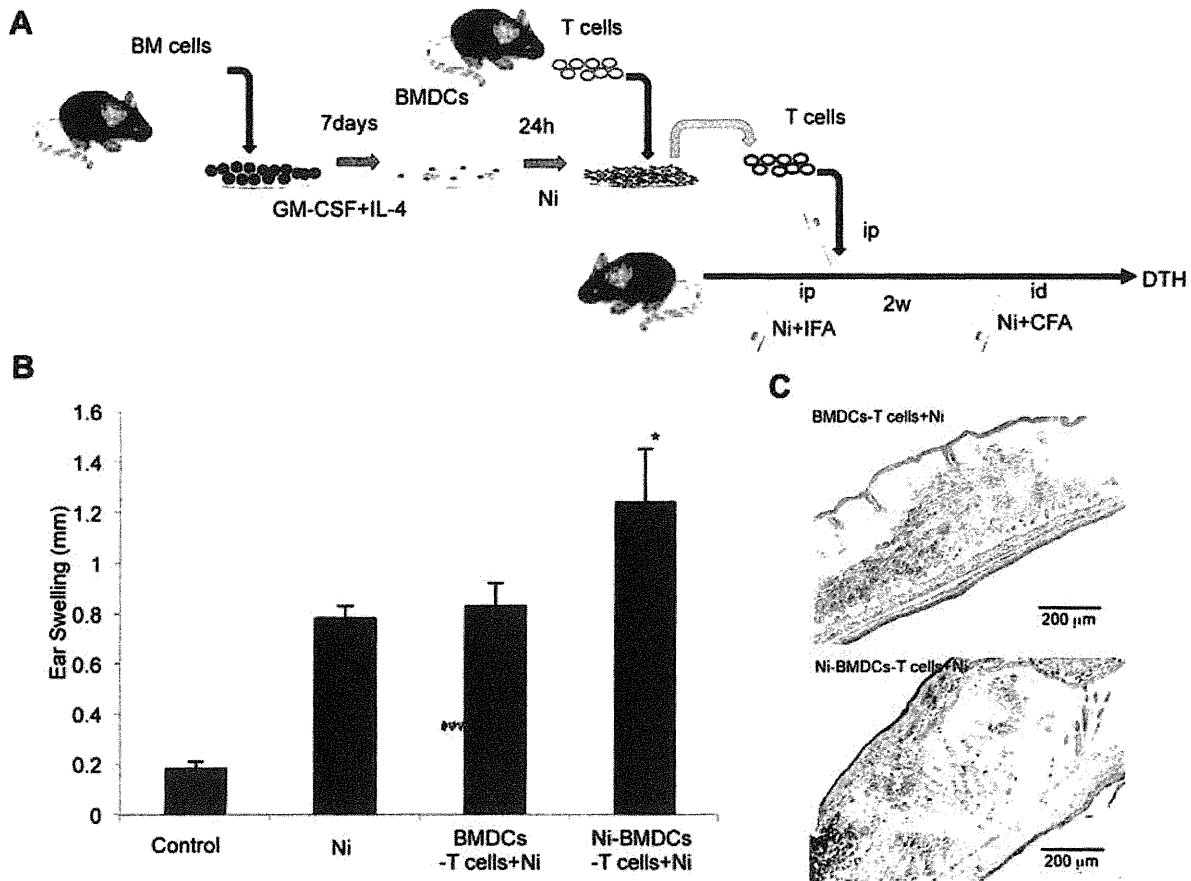


**Figure 4. Effect of T cell transfer on DTH in the Ni allergy model.** (A) Purified T cells from the spleens of B6 mice were co-cultured with BMDCs in the absence (control) or presence of  $\text{NiCl}_2$  for 48 hours and then intraperitoneally transferred into B6 mice. DTH reaction was induced by injecting  $\text{NiCl}_2$ . (B) Ear thickness was measured at 48 hours after the challenge. Results are means  $\pm$  SD for 5 mice in each group. \* $P < 0.05$ . (C) Inflammatory lesions of the mice with transferred Ni-DC-stimulated T cells. doi:10.1371/journal.pone.0019017.g004

It was recently reported that human Toll-like receptor (TLR) 4 plays a crucial role in the development of contact allergy to Ni [37] and that only TLR4-deficient mice expressing transgenic human TLR4 developed contact hypersensitivity to Ni, while animals expressing mouse TLR4 did not develop DTH. Although the cell type contributing to a TLR4-mediated allergic reaction was not identified, immune cells such as DCs, macrophages, and endothelial cells were associated with an allergic reaction to Ni via TLR4. It is possible that TLRs other than TLR4 are related to Ni allergy in mice. In our mouse model, although the signaling pathway via TLR in DCs was not examined, MKK6 phosphorylation was observed in LPS-stimulated DCs *in vitro*. Thus, cooperative or synergistic actions of Ni with other signaling pathways, including TLR, following MKK6 activation may be associated with Ni allergy in this mouse model. Our *in vivo* experiments suggested that DCs activated by Ni enhanced T cell migration to local lesions and T cell-dependent allergic response; however, it remains unclear how Ni can stimulate or control DC activation via MKK6. Moreover, our result showed that significantly increased number of NKT cells reactive to anti- $\alpha\text{GalCer-CD1d}$  complex was found in the ear lesion of Ni model mice. CD1d-restricted NKT cells have been referred to as natural memory cells in both innate and acquired immune responses [38]. However, the relationship between metal allergy and the role of NTK cell has been still unidentified. Further research using our

model will be necessary for understanding the cellular mechanism of metal allergy.

DC maturation can be initiated by inflammatory stimuli, such as cytokines, LPS, CD40 ligation, and contact allergens [39]. Activated DCs take up antigens and produce a variety of cytokines and chemokines, which in turn attract and activate eosinophils, macrophages, and NK cells to the site of antigen entry [30]. After antigen capture, DCs migrate to regional lymph nodes and present peptide-MHC complexes to antigen-specific T cells that induce T cell-dependent immune responses, such as Ni allergy [40]. Interestingly, our results showed a significantly increased number of dermal DCs in the skin tissues of mice with Ni allergy. These findings suggest that circulating precursor DCs might accumulate at the  $\text{NiCl}_2$  injection site. Moreover, the experiments using skin tissues demonstrated that phosphorylation of MKK6 in dermal DCs and LCs was clearly detectable. These results indicated that stimulation with Ni enhanced both accumulation and activation of DCs.

DCs are activated by signaling via pattern recognition receptors (PRRs), such as TLRs and retinoic acid-inducible gene I-like receptors, in response to a variety of ligands [41,42]. PRR signaling leads to the activation of nuclear factor (NF)- $\kappa\text{B}$ . Although it is unclear whether Ni can interact with receptors such as PRRs, previous reports showed that the differentiation of human DCs is promoted by Ni via NF- $\kappa\text{B}$  activation [43,44]. It

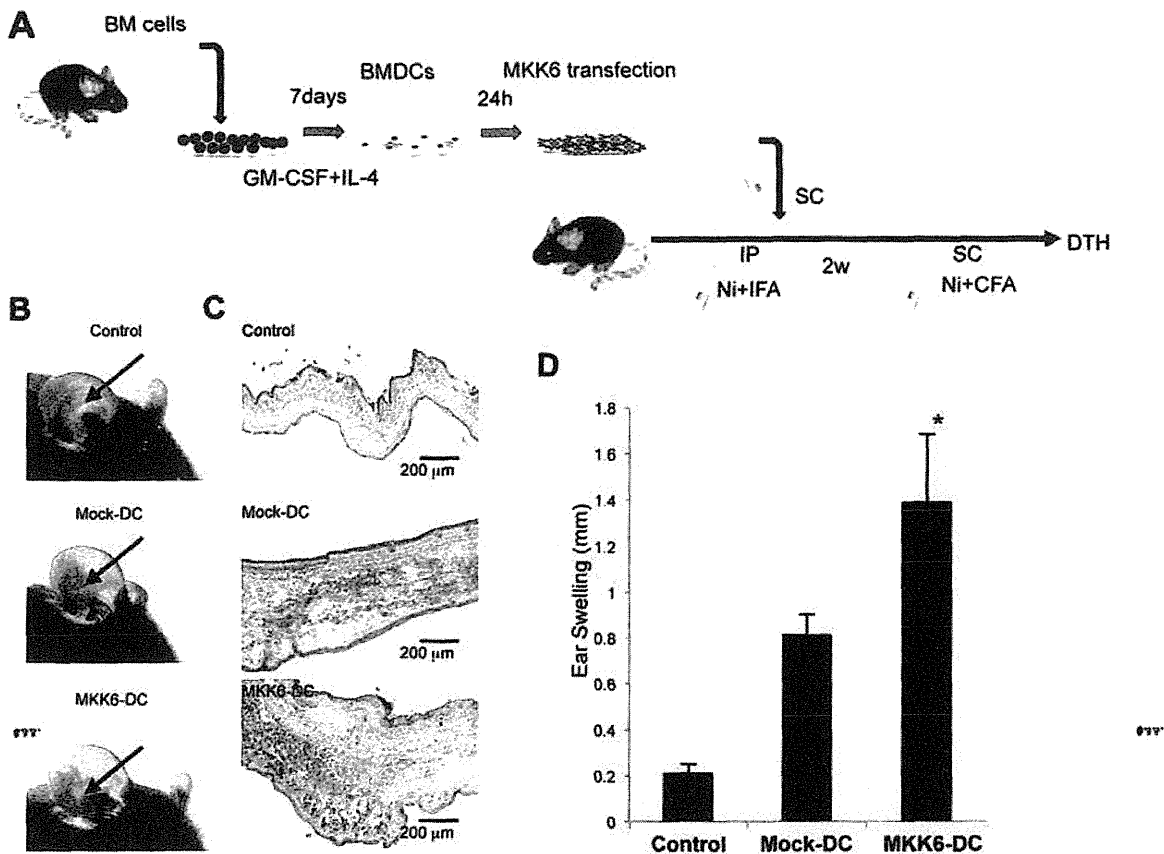


**Figure 5. Effect of DC transfer on the Ni allergy reaction.** (A) MKK6 DNA or mock plasmids were transfected into BMDCs. MKK6/DCs or Mock/DCs were subcutaneously injected into B6 mice. The mice were challenged with NiCl<sub>2</sub> to induce DTH. (B) Representative photos are shown for 3 to 5 mice in each group. (C) Inflammatory lesions of the mice with transferred MKK6/DCs. These results are representative of 2 independent experiments with 3 mice in each group. (D) Ear thickness was measured at 48 hours after the challenge. Results are means  $\pm$  SD for 5 mice in each group. \* $P < 0.05$ . doi:10.1371/journal.pone.0019017.g005

remains uncertain whether NF- $\kappa$ B signaling plays a role in the pathogenesis of metal allergy.

Our *in vivo* experiments demonstrated that manipulating the MKK6 gene of DCs could control Ni allergy. Many reports on DC therapy for cancer or infection have indicated that antigen presentation to T cells by DCs is important for controlling these diseases [14,45,46]. However, there are no reports regarding DC therapy for metal allergy. Our new approach with siRNA targeting the MKK6 gene could be a powerful strategy for the prevention and cure of metal allergy. Careful attention should be paid to the therapeutic effects of MKK6 inhibition on the immune system in the treatment of allergic immune responses.

In conclusion, the signaling pathway via p38/MKK6 plays a key role in activating dermal DCs in the pathogenesis of metal allergy. DC therapy using MKK6 gene manipulation could be effective for treating metal allergy. Characterization of this cellular mechanism could have clinical implications by supporting the development of new diagnoses or treatments for these allergic diseases.

## Materials and Methods

### Ethics

This study was conducted according to the principles expressed in the Declaration of Helsinki. The study was approved by the

Institutional Review Board of the University of Tokushima (toku09021).

### Mice

Female C57BL/6J mice (6–8 weeks old) were purchased from CLEA Japan, Inc (Tokyo, Japan). All mice were maintained in specific pathogen-free conditions in our animal facility.

### Histology and Immunohistochemistry

Skin was removed from the mice, fixed with 10% phosphate-buffered formaldehyde (pH 7.2), and prepared for histological examination. Formalin-fixed tissue sections were stained with hematoxylin and eosin. Immunohistochemistry was performed for freshly frozen sections by the biotin-avidin immunoperoxidase method using an avidin-biotin immunoperoxidase complex reagent (Vector Laboratories, Burlingame, CA, USA). Monoclonal antibodies against CD3 and CD19 (eBioscience, San Diego, CA, USA) were used.

### Induction of Ni Allergy

Ni allergy was induced using a modification of a method described previously [24,25]. To induce a hypersensitivity reaction to Ni, 25  $\mu$ l of 1  $\mu$ mol/ml NiCl<sub>2</sub> with 25  $\mu$ l of IFA (ICN Biomedicals, Inc., Aurora, OH, USA) was intraperitoneally injected into B6 mice for initial immunization. Two weeks later, mice were administered intradermal injections of Ni,

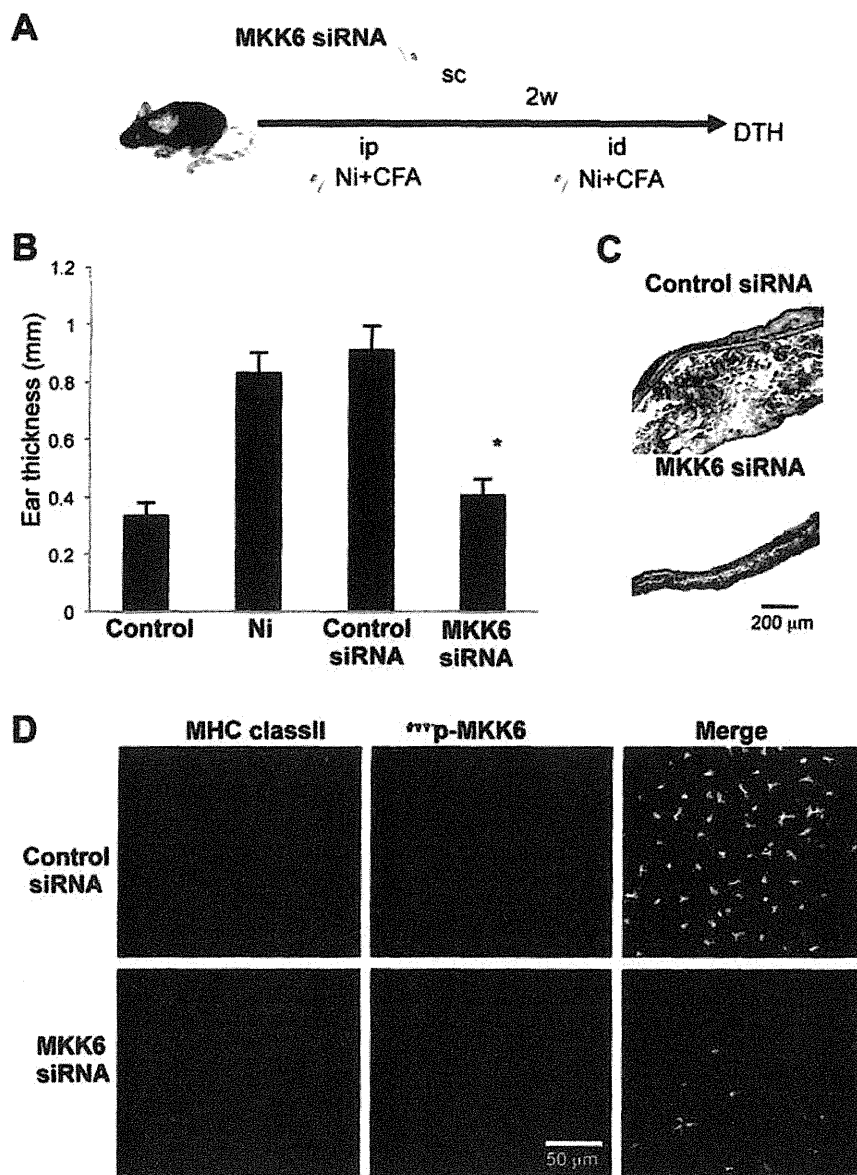


**Figure 6. DC therapy for Ni allergy.** (A) siRNA for MKK6 with atelocollagen was subcutaneously injected into the ear skin of Ni allergy mice. (B) Ear thickness was measured at 48 hours after injecting NiCl<sub>2</sub>. Results are means  $\pm$  SD for 5 mice in each group. \* $P < 0.05$ . (C) Pathological findings after *in vivo* administration of MKK6 siRNA and control siRNA. (D) Phosphorylation of MKK6 of MHC class II<sup>+</sup> dermal DCs was analyzed by confocal microscopy. These results are representative of experiments with 5 mice in each group. doi:10.1371/journal.pone.0019017.g006

10  $\mu$ l of 0.2  $\mu$ mol/ml NiCl<sub>2</sub> with CFA (ICN Biomedicals, Inc.) using 28G1/2 needles (TERUMO Tokyo, Japan) for a recall immune response. DTH reactions were determined by measuring the changes in ear thickness at 24 or 48 hours after the challenge [25].

#### DC Preparation

DCs were prepared from freshly isolated bone marrow cells as described previously [26]. Briefly, bone marrow cells were seeded in 6-well culture plates (Nunc A/S, Roskilde, Denmark) in RPMI-1640 medium supplemented with 10% heat-inactivated FCS, 2 mM L-glutamine, 100 U/ml penicillin, and 100  $\mu$ g/ml streptomycin, and then incubated for 1 hour at 37°C in a humidified 5% CO<sub>2</sub> atmosphere. After nonadherent cells were

removed, adherent cells were incubated and changed to 1 ml of fresh medium containing 10 ng/ml GM-CSF (R&D System, Inc., Minneapolis, MN, USA) and 1 ng/ml IL-4 (eBioscience) on days 2, 4, and 6. Dermal DCs were prepared from the skin of female B6 mice. Excised skin was cut into small pieces and the dermal side was exposed to 1.0% trypsin at 37°C for 60 minutes. Epidermis was incubated in 0.025% DNase for 20 minutes at room temperature. After an equal volume of RPMI was added, the solution was swirled for 5 minutes and filtered using a 70  $\mu$ m cell strainer (BD Biosciences, Franklin Lakes, NJ, USA). The dermal cell suspension that included DCs was washed three times with RPMI, and the resulting pellet was re-suspended. Dermal DCs were enriched by centrifugation using Opti-prep (Invitrogen, Carlsbad, CA, USA).

## Flow Cytometry

Expression levels of surface markers were examined by staining  $1 \times 10^6$  cells with 1  $\mu\text{g}/\text{ml}$  of antibodies against CD3, CD4, CD8, CD19, CD11c, and MHC class II conjugated with either FITC or PE (eBioscience). Cells were analyzed on FACScan (BD Biosciences).

## Western Blot Analysis

Samples of stimulated or nonstimulated DCs were subjected to sodium dodecyl sulfate-polyacrylamide gel electrophoresis (SDS-PAGE) with 10% acrylamide gel, transferred onto a polyvinylidene fluoride (PVDF) membrane (Bio-Rad Laboratories, Hercules, CA, USA), and the blotted membranes were incubated with anti-MKK6, phospho-MKK6 (Cell Signaling Technology, Inc., Denver, MA, USA), or glyceraldehyde-3-phosphate dehydrogenase (GAPDH) (Santa Cruz Biotechnology, Inc., Santa Cruz, CA, USA) mAbs. Immune complexes were detected using horseradish peroxidase (HRP)-conjugated anti-mouse IgG (Bio-Rad Laboratories) and ECL-plus reagents (Amersham Bioscience Corp. Piscataway, NJ, USA).

## MKK6 Plasmid Construction and Transfection

MKK6 cDNA obtained from RT-PCR was subcloned into an expression vector, pcDNA3.1 (Invitrogen). Transient transfections were carried out using a jet-PEI Mannose reagent (Polytransfection, Illkirch, France) before stimulation. DCs were transfected with the MKK6 plasmid, and then stimulated with either 1  $\mu\text{mol}/\text{ml}$   $\text{NiCl}_2$  or 1  $\mu\text{mol}/\text{ml}$   $\text{TiO}_2$  for 48 hours.

## siRNA for MKK6

MKK6 and control scramble siRNA reagents were obtained from B-bridge International, Inc. (Sunnyvale, CA, USA). Sequences of the oligonucleotides were as follows: MKK6: sense, 5'-CUACAGUAGUGAAGAGAUUTT-3'; antisense, 5'-AAUCUCUUCACUACUGUAGTT-3' and control: 5'-ATCCGCGCGATAGTACGTA-3'. Using the *in vivo* siRNA transfection kit AteloGene (KOKEN, Tokyo, Japan), siRNA was injected into ear skin according to the manufacturer's instructions [47]. In brief, 10  $\mu\text{M}$  siRNA was mixed with AteloGene and rotated gently at 4°C for 20 minutes. This solution (20  $\mu\text{l}$ ) was subcutaneously injected into the ear pinnae. Five days after injection, ear swelling was evaluated.

## Confocal Microscopic Analysis

Skin sheets were isolated from ears of treated mice with 3.8% ammonium thiocyanate, and stained with anti-phospho-MKK6 (Santa Cruz Biotechnology) mAb and MHC class II mAb (eBioscience). These sheets were analyzed using Confocal Laser Microscan (LSM 5 PASCAL; Carl Zeiss, Inc., Oberkochen, Germany).

## Statistical Analysis

Results are given as means  $\pm$  standard deviations (SD). Comparison was done using Student's *t* test or Mann-Whitney *U* test. Differences were considered statistically significant for *P* values of  $<0.05$ .

## Supporting Information

**Figure S1** Inflammatory lesions in Ni allergy model. (A) Edema and inflammatory cell infiltrations were observed in the skin tissues

of Ni allergy mice. Photos are representative of five mice in each group. Original magnification is  $\times 100$  (upper) and  $\times 200$  (lower). (B) The number of toluidine blue<sup>+</sup> cells including mast cell in the lesion of Ni allergy model was significantly increased compared to that of control mice. Toluidine blue staining was performed as described in Methods S1. Photos are representative of three mice in each group. Data are means  $\pm$  SD of 3 mice. \**P* $<0.05$ , vs control.

(TIF)

**Figure S2** Flow cytometric analysis of immune cells in Ni allergy model. (A)  $\text{CD4}^+$  and  $\text{CD8}^+$  T cells or  $\text{NK1.1}^+$  cells of ear tissues from controls and Ni allergy models were detected by flow cytometry. Results are representative of three mice in each group. (B) NKT cells of spleen, cervical lymph nodes, and ear tissues were detected by using PE-conjugated anti- $\alpha\text{GalCer}$  mAb- $\text{CD1d}$  complex. Results are representative of three mice in each group. (C)  $\text{CD11c}^+$  MHC class II<sup>+</sup> DCs in cervical lymph nodes (LNs) from control, OVA,  $\text{TiO}_2$ , and  $\text{NiCl}_2$ -injected mice were analyzed by flow cytometry as described in Method S1. The results were representative of three to five mice in each group.

(TIF)

**Figure S3** Activation of MAPK signaling of DCs by Ni. (A) BMDCs were stimulated with  $\text{NiCl}_2$ , LPS or  $\text{TiO}_2$  for 24 hours, phosphorylation of MKK6 and p38, and total MKK6 and p38 protein were detected by Western blot analysis. GAPDH was used as the respective internal control. Results are representative of 3 independent experiments. (B) MKK6 mRNA expression of BMDCs stimulated with  $\text{NiCl}_2$  or LPS was analyzed by real-time PCR as described in Method S1. Data are shown as relative expressions to  $\beta$ -actin, and are representative of 3 independent experiments.

(TIF)

**Figure S4** Cytokine secretions from Ni-stimulated T cells. T cells from cLNs of control, OVA,  $\text{TiO}_2$ , and  $\text{NiCl}_2$ -injected mice were enriched by negative selection using mAbs (anti-MHC class II, B220, NK1.1, and CD11b) and magnetic beads. The T cells were stimulated with plate-coated anti-CD3 mAb for 24 hours. The secretions of IL-2, IFN- $\gamma$ , IL-4, and IL-10 in the supernatants were analyzed by ELISA as described in Method S1. Data are means  $\pm$  SD of triplicates. \**P* $<0.05$ , vs control.

(TIF)

**Figure S5** Cytokine secretions from Ni-stimulated DCs. BMDCs were stimulated with  $\text{NiCl}_2$ , LPS, and  $\text{TiO}_2$  for 24 hours. The cytokine secretions of IL-12, IFN- $\gamma$ , and IL-10 were detected by ELISA as described in Method S1. Data are means  $\pm$  SD of triplicates.

(TIF)

## Methods S1

(DOCX)

## Acknowledgments

We thank S. Katada, A. Nagaoka, and N. Kino for their technical assistance.

## Author Contributions

Conceived and designed the experiments: MW NI TI YH. Performed the experiments: MW NI MNA RA AY. Analyzed the data: MW NI MNA. Wrote the paper: MW NI YH.

## References

1. Forte G, Petrucci F, Bocca B (2008) Metal allergens of growing significance: epidemiology, immunotoxicology, strategies for testing and prevention. *Inflamm Allergy Drug Targets* 7: 145–162.
2. Nosbaum A, Vocanson M, Rozieres A, Hennino A, Nicolas JF (2009) Allergic and irritant contact dermatitis. *Eur J Dermatol* 19: 325–332.
3. Budinger L, Hertl M (2000) Immunologic mechanisms in hypersensitivity reactions to metal ions: an overview. *Allergy* 55: 108–115.
4. Martin SF, Jakob T (2008) From innate to adaptive immune responses in contact hypersensitivity. *Curr Opin Allergy Clin Immunol* 8: 289–293.
5. Basketter DA, Briatico-Vangosa G, Kaestner W, Lally C, Bontinck WJ (1993) Nickel, cobalt and chromium in consumer products: a role in allergic contact dermatitis? *Contact Dermatitis* 28: 15–25.
6. Aberer W, Holub H, Strohhal R, Slavicek R (1993) Palladium in dental alloys—the dermatologists' responsibility to warn? *Contact Dermatitis* 28: 163–165.
7. Rustemeyer T, von Blomberg BM, van Hoogstraten IM, Bruynzeel DP, Scheper RJ (2004) Analysis of effector and regulatory immune reactivity to nickel. *Clin Exp Allergy* 34: 1458–1466.
8. Sinigaglia F, Scheidegger D, Garotta G, Scheper R, Pletscher M, et al. (1958) Isolation and characterization of Ni-specific T cell clones from patients with Ni-contact dermatitis. *J Immunol* 135: 3929–3932.
9. Kapsenberg ML, Wierenga EA, Stiekema FE, Tiggeleman AM, Bos JD (1992) Th1 lymphokine production profiles of nickel-specific CD4+T-lymphocyte clones from nickel contact allergic and non-allergic individuals. *J Invest Dermatol* 98: 59–63.
10. Moed H, Boorsma DM, Stoof TJ, von Blomberg BM, Bruynzeel DP, et al. (2004) Nickel-responding T cells are CD4+ CLA+ CD45RO+ and express chemokine receptors CXCR3, CCR4 and CCR10. *Br J Dermatol* 151: 32–41.
11. Banchereau J, Steinman RM (1998) Dendritic cells and the control of immunity. *Nature* 392: 245–252.
12. Steinman RM, Banchereau J (2007) Taking dendritic cells into medicine. *Nature* 449: 419–426.
13. Mortz CG, Lauritsen JM, Bindsvlev-Jensen C, Andersen KE (2001) Prevalence of atopic dermatitis, asthma, allergic rhinitis, and hand and contact dermatitis in adolescents. The Odense Adolescence Cohort Study on Atopic Diseases and Dermatitis. *Br J Dermatol* 144: 523–532.
14. Thierse HJ, Gernerding K, Junkes C, Guerreiro N, Weltzien HU (2005) T cell receptor (TCR) interaction with haptens: metal ions as non-classical haptens. *Toxicology* 209: 101–107.
15. Roake JA, Rao AS, Morris PJ, Larsen CP, Hankins DF, et al. (1995) Dendritic cell loss from nonlymphoid tissues after systemic administration of lipopolysaccharide, tumor necrosis factor, and interleukin 1. *J Exp Med* 181: 2237–2247.
16. Lore K, Sonnerborg A, Spetz A L, Andersson U, Andersson J (1998) Immunocytochemical detection of cytokines and chemokines in Langerhans cells and in vitro derived dendritic cells. *J Immunol Methods* 218: 173–187.
17. Riedl E, Stockl J, Majdic O, Scheinecker C, Knapp W, et al. (2000) Ligation of E-cadherin on in vitro-generated immature Langerhans-type dendritic cells inhibits their maturation. *Blood* 96: 4276–4284.
18. Geissmann F, Dieu-Nosjean MC, Dezutter C, Valladeau J, Kayal S, et al. (2002) Accumulation of immature Langerhans cells in human lymph nodes draining chronically inflamed skin. *J Exp Med* 196: 417–430.
19. Villadangos JA, Cardoso M, Steptoe RJ, van Berkel D, Pooley J, et al. (2001) MHC class II expression is regulated in dendritic cells independently of invariant chain degradation. *Immunity* 14: 739–749.
20. Verhasselt V, Buelens C, Willems F, De Groot D, Haeflner-Cavaillon N, et al. (1997) Bacterial lipopolysaccharide stimulates the production of cytokines and the expression of costimulatory molecules by human peripheral blood dendritic cells: evidence for a soluble CD14-dependent pathway. *J Immunol* 158: 2919–2925.
21. Kyriakis JM, Avruch J (2001) Mammalian mitogen-activated protein kinase signal transduction pathways activated by stress and inflammation. *Physiol Rev* 81: 807–869.
22. Arrighi JF, Rebsamen M, Rousset F, Kindler V, Hauser C (2001) A critical role for p38 mitogen-activated protein kinase in the maturation of human blood-derived dendritic cells induced by lipopolysaccharide, TNF- $\alpha$ , and contact sensitizers. *J Immunol* 166: 3837–3845.
23. Jorgl A, Platzer B, Taschner S, Heinz LX, Hocher B, et al. (2007) Human Langerhans-cell activation triggered in vitro by conditionally expressed MKK6 is counterregulated by the downstream effector RelB. *Blood* 109: 185–193.
24. Nakae S, Naruse-Nakajima C, Sudo K, Horai R, Asano M, et al. (2001) IL-1 $\alpha$ , but not IL-1 $\beta$ , is required for contact-allergen-specific T cell activation during the sensitization phase in contact hypersensitivity. *Int Immunol* 13: 1471–1478.
25. Artik S, von Vultee C, Gleichmann E, Schwarz T, Griem P (1999) Nickel allergy in mice: enhanced sensitization capacity of nickel at higher oxidation states. *J Immunol* 163: 1143–1152.
26. Black J (1999) Allergic foreign body response. In: *Biological performance of materials – Fundamentals of biocompatibility*, 3<sup>rd</sup> edition. New York and Basel Marcel Dekker. pp 215–232.
27. Fields RC, Shimizu K, Mule JJ (1998) Murine dendritic cells pulsed with whole tumor lysates mediate potent antitumor immune responses in vitro and in vivo. *Proc Natl Acad Sci U S A* 95: 9482–9487.
28. Banchereau J, Briere F, Caux C, Davoust J, Lebecque S, et al. (2000) Immunobiology of dendritic cells. *Annu Rev Immunol* 18: 767–811.
29. Nakahara T, Moroi Y, Uchi H, Furue M (2006) Differential role of MAPK signaling in human dendritic cell maturation and Th1/Th2 engagement. *J Dermatol Sci* 42: 1–11.
30. Toebak MJ, Gibbs S, Bruynzeel DP, Scheper RJ, Rustemeyer T (2009) Dendritic cells: biology of the skin. *Contact Dermatitis* 60: 2–20.
31. Bennett CL, Noordegraaf M, Martina CA, Clausen BE (2007) Langerhans cells are required for efficient presentation of topically applied hapten to T cells. *J Immunol* 179: 6830–6835.
32. Rincon M, Davis RJ (2009) Regulation of the immune response by stress-activated protein kinases. *Immunol Rev* 228: 212–224.
33. Brown MD, Sacks DB (2009) Protein scaffolds in MAP kinase signalling. *Cell Signal* 21: 462–469.
34. Boislevé F, Kerdine-Romer S, Pallardy M (2005) Implication of the MAPK pathways in the maturation of human dendritic cells induced by nickel and TNF- $\alpha$ . *Toxicology* 206: 233–244.
35. Miyazawa M, Ito Y, Kosaka N, Nukada Y, Sakaguchi H, et al. (2008) Role of MAPK signaling pathway in the activation of dendritic type cell line, THP-1, induced by DNCB and NiSO<sub>4</sub>. *J Toxicol Sci* 33: 51–59.
36. Trompezinski S, Migdal C, Tailhardat M, Le Varlet B, Courtellemont P, et al. (2008) Characterization of early events involved in human dendritic cell maturation induced by sensitizers: cross talk between MAPK signalling pathways. *Toxicol Appl Pharmacol* 230: 397–406.
37. Schmidt M, Raghavan B, Muller V, Vogl T, Fejer G, et al. (2010) Crucial role for human Toll-like receptor 4 in the development of contact allergy to nickel. *Nat Immunol* 11: 814–819.
38. Thomas SY, Hou R, Boyson JE, Means TK, Hess C, et al. (2003) CD1d-restricted NKT cells express a chemokine receptor profile indicative of Th1-type inflammatory homing cells. *J Immunol* 171: 2571–2580.
39. Aiba S, Terunuma A, Manome H, Tagami H (1997) Dendritic cells differently respond to haptens and irritants by their production of cytokines and expression of co-stimulatory molecules. *Eur J Immunol* 27: 3031–3038.
40. Cavani A, Nasorri F, Prezzi C, Sebastiani S, Albanesi C, et al. (2000) Human CD4+ T lymphocytes with remarkable regulatory functions on dendritic cells and nickel-specific Th1 immune responses. *J Invest Dermatol* 114: 295–302.
41. Van Waes C (2007) Nuclear factor- $\kappa$ B in development, prevention, and therapy of cancer. *Clin Cancer Res* 13: 1076–1082.
42. Kaisho T, Tanaka T (2008) Turning NF- $\kappa$ B and IRFs on and off in DC. *Trends Immunol* 29: 329–336.
43. Ade N, Antonios D, Kerdine-Romer S, Boislevé F, Rousset F, et al. (2007) NF- $\kappa$ B plays a major role in the maturation of human dendritic cells induced by NiSO<sub>4</sub> but not by DNCB. *Toxicol Sci* 99: 488–501.
44. Antonios D, Ade N, Kerdine-Romer S, Assaf-Vandecasteele H, Larange A, et al. (2009) Metallic haptens induce differential phenotype of human dendritic cells through activation of mitogen-activated protein kinase and NF- $\kappa$ B pathways. *Toxicol In Vitro* 23: 227–234.
45. O'Neill D, Bhardwaj N (2005) Exploiting dendritic cells for active immunotherapy of cancer and chronic infection. *Methods Mol Med* 109: 1–18.
46. Koski GK, Cohen PA, Roses RE, Xu S, Czerniecki BJ (2008) Reengineering dendritic cell-based anti-cancer vaccines. *Immunol Rev* 222: 256–276.
47. Kinouchi N, Ohsawa Y, Ishimaru N, Ohuchi H, Sunada Y, et al. (2008) Atelocollagen-mediated local and systemic applications of myostatin-targeting siRNA increase skeletal muscle mass. *Gene Ther* 15: 1126–1130.

1 Unique Roles of Estrogen-Dependent Pten Control in Epithelial Cell Homeostasis of  
2 Mouse Vagina

3

4 Shinichi Miyagawa<sup>1</sup>, Masaru Sato<sup>1</sup>, Tamotsu Sudo<sup>2</sup>, Gen Yamada<sup>3</sup>, Taisen Iguchi<sup>1,\*</sup>

5

6 <sup>1</sup>Okazaki Institute for Integrative Bioscience, National Institute for Basic Biology,  
7 National Institutes of Natural Sciences, and Department of Basic Biology, The Graduate  
8 University for Advanced Studies, Okazaki, Aichi 444-8787, Japan

9

10 <sup>2</sup>Section of Translational Research and Department of Gynecologic Oncology, Hyogo  
11 Cancer Center, Akashi, Hyogo 673-8558, Japan

12

13 <sup>3</sup>Department of Developmental Genetics and Laboratory Animal Center, Institute of  
14 Advanced Medicine, Wakayama Medical University, Wakayama, Wakayama 641-8509,  
15 Japan

16

17 \*Correspondence: Taisen Iguchi, National Institute for Basic Biology, Okazaki

18 444-8787, Japan

19 E-mail: taisen@nibb.ac.jp

20 Phone: +81-564-59-5235, Fax: +81-564-59-5236

21

22 **Keywords:** Vagina, Pten, Akt, Estrogen, Epithelium

23

24 **Short title:** Pten function in vagina



25

26 **Abbreviations;** Akt, v-akt murine thymoma viral oncogene homolog; CAH; complex  
27 atypical hyperplasia, CK; cytokeratin, CKO; conditional knock-out, E2, 17 $\beta$ -estradiol;  
28 EGF, epidermal growth factor; ER, estrogen receptor; IGF, insulin-like growth factor,  
29 MAPK, mitogen-activated protein kinase; mTOR, mammalian target of rapamycin;  
30 OVX, ovariectomy; PI3K, phosphoinositide-3-kinase; PTEN, phosphatase and tensin  
31 homolog deleted from chromosome 10; PIP<sub>3</sub>, phosphatidylinositol 3,4,5-trisphosphate;  
32 PIP<sub>2</sub>, phosphatidylinositol 4,5-bisphosphate

33

34 **Abstract**

35           Numerous studies support a role of Phosphatase and tensin homolog deleted  
36 from chromosome 10 (Pten) as a tumor suppressor gene that controls epithelial cell  
37 homeostasis to prevent tumor formation. Mouse vaginal epithelium cyclically exhibits  
38 cell proliferation and differentiation in response to estrogen and provides a unique  
39 model for analyzing homeostasis of stratified squamous epithelia. We analyzed vaginal  
40 epithelium-specific *Pten* conditional knock-out (CKO) mice to provide new insights  
41 into Pten/phosphoinositide-3-kinase (PI3K)/Akt function. The vaginal epithelium of  
42 ovariectomized (OVX) mice (control) was composed of 1-2 layers of cuboidal cells,  
43 while OVX CKO mice exhibited epithelial hyperplasia in the suprabasal cells with  
44 increased cell mass and mucin production. This is possibly due to misactivation of  
45 mammalian target of rapamycin (mTOR) and mitogen-activated protein kinase (MAPK).  
46 Intriguingly, estrogen administration to OVX *Pten* CKO mice induced stratification and  
47 keratinized differentiation in the vaginal epithelium as in estrogen-treated controls. We  
48 found Pten is exclusively expressed in the suprabasal cells in the absence of estrogens,  
49 whereas estrogen administration induced Pten expression in the basal cells. This  
50 suggests that Pten acts to prevent excessive cell proliferation as in the case for other  
51 squamous tissues. Thus, Pten exhibits a dual role on the control of vaginal homeostasis,  
52 dependent on whether estrogens are present or absent. Our results provide new insights  
53 into how Pten functions in tissue homeostasis.

54

55 **Introduction**

56           Phosphatase and tensin homolog deleted from chromosome 10 (*Pten*) is a  
57 lipid phosphatase that functions as a tumor-suppressor, and mutations in *Pten* are  
58 frequently found both in sporadic and hereditary cancers. *Pten* acts in opposition to  
59 phosphatidylinositol 3-kinase (PI3K) function. In the absence of *Pten* activity,  
60 concentrations of phosphatidylinositol 3,4,5-trisphosphate (PIP<sub>3</sub>), a lipid second  
61 messenger produced by PI3K, are increased, leading to enhancement of phosphorylation  
62 and activation of the v-akt murine thymoma viral oncogene homolog (Akt). Akt kinase  
63 activity exerts anti-apoptotic and pro-proliferative functions; therefore, mice with *Pten*  
64 deletion and/or loss-of-function mutations are highly susceptible to tumor induction by  
65 abnormal Akt activation. *Pten* plays a pivotal role in maintaining stratified squamous  
66 epithelia because conditional knockout of *Pten* in the epithelium leads to hyperplasia,  
67 hyperkeratosis, and tumor formation in skin, esophagus and stomach <sup>1</sup>.

68           Cell proliferation and differentiation of stratified squamous epithelia must be  
69 tightly regulated and coordinated during homeostasis. Vaginal epithelium, despite its  
70 similarity to other stratified squamous epithelia, is exceptional in one major way - the  
71 vaginal epithelium exhibits cyclical, estrogen-dependent cell proliferation and  
72 differentiation during the estrous cycle. The vaginae of ovariectomized (OVX) mice  
73 contain an atrophied epithelium of 2-3 cell layers; estrogen administration rapidly  
74 induces epithelial cell proliferation in the basal layer. The suprabasal cells are no longer  
75 mitogenic but differentiate while moving up through the epithelium. Apical cells exhibit  
76 keratinization. The fully stratified and keratinized vaginal epithelium resembles the  
77 typical stratified and keratinized epidermis found in the skin and other organs. Thus, the  
78 vaginal epithelium provides a unique model to study homeostasis in stratified squamous

79 epithelia. There are several case reports of vaginal cysts in the patients with Cowden's  
80 disease, which is associated with *Pten* mutation<sup>2,3</sup>. In addition, there is one reported  
81 description of a vaginal squamous cell carcinoma in *Pten* mutant mice<sup>4</sup>. However, little  
82 is known about the usual function of Pten/PI3K/Akt signaling or its relationship with  
83 estrogen signaling in the vagina.

84           In rodent reproductive organs such as vagina and uterus, the effects of  
85 estrogen on the epithelia are mediated primarily via stromally expressed estrogen  
86 receptor  $\alpha$  (ER $\alpha$ )<sup>5,6</sup>. Estrogen-induced growth factors secreted from the stroma  
87 promote epithelial cell proliferation<sup>7</sup>, resulting in activation of cellular signal  
88 transduction via PI3K/Akt and mitogen-activated protein kinase (MAPK) signaling  
89 cascades<sup>8,9</sup>. Epidermal growth factor (EGF)-like growth factors and insulin-like growth  
90 factor (IGF)-I have mitogenic effects similar to estrogens and administration of these  
91 growth factors to OVX adult mice induced cell proliferation and differentiation in the  
92 female reproductive tract<sup>10-12</sup>. These results suggest that Akt and MAPK signalings are  
93 functional mediators of estrogen-induced cell proliferation and differentiation.  
94 Importantly, aberrant PI3K/Akt activation results in complex atypical hyperplasia and  
95 endometrioid carcinoma in the uterus<sup>13-16</sup>. Therefore, repression of PI3K/Akt signaling  
96 is considered to be essential during the absence of estrogen in the vagina as well.

97           In the present study, we analyzed epithelium-specific *Pten* conditional  
98 knock-out (CKO) mouse vagina to provide new insights into Pten/PI3K/Akt function.  
99 We found that Pten is expressed in suprabasal epithelial cells where it prevents  
100 abnormal cell proliferation and differentiation in the absence of estrogen. On the other  
101 hand, in the presence of estrogen, Pten is predominantly expressed in basal epithelial  
102 cells, where it may aid in preventing tumor induction. Thus, Pten exhibits a dual role on